Interanionic $^{(-)}O-H\cdots O^{(-)}$ Interactions: A Solid-State and Computational Study of the Ring and Chain Motifs

Dario Braga,*[a] Lucia Maini,[a] Fabrizia Grepioni,*[b] Fernando Mota,[c] Carme Rovira,[c] and Juan J. Novoa[c][+]

Abstract: The $^{(-)}O-H\cdots O^{(-)}$ interaction formed by the anions HCO_3^-, $HC_2O_4^-$, $HC_4O_4^-$ and $HC_5O_5^-$ (HA^-), obtained upon monodeprotonation of the corresponding carbonic, oxalic, squaric and croconic acids (H_2A), has been investigated theoretically and experimentally. The ring (RING) and chain (CHAIN) hydrogen bond motifs established between these anions have been analysed in terms of geometry and energy and their occurrence in crystalline salts investigated by searching the Cambridge Structural Database (CSD) and the Inorganic Chemistry Structural Database (ICSD). It has been shown that hydrogen carbonates form RINGs, with the notable exception of $NaHCO_3$, while only CHAINs are known for hydrogen oxalates. Hydrogen squarates and hydrogen croconates can form both RINGs and CHAINs. The structures of Rb^+ and Cs^+ hydrogen croconates, which present the two alternative motifs, have been discussed together with that of the hydrated salt $NaHC_5O_5\cdot H_2O$. The relationship between RING and CHAIN has been examined in the light of ab initio calculations. A rigorous quantum chemical study of the nature of the interanionic $^{(-)}O-H\cdots O^{(-)}$ interaction in both vacuum and condensed phase has shown that the interaction energy is dominated by the electrostatic component which becomes attractive at short $O\cdots O$ distances (less than 2.5 Å) if the net ionic charge on the anion is delocalised away from the $-OH$ group. It has been demonstrated that the RING motif is slightly metastable with respect to dissociation in the gas phase, but becomes stable in the crystal owing to the influence of the Madelung field. However, the CHAIN motif is unstable both in the gas phase and in the crystal. It is argued that interanionic $^{(-)}O-H\cdots O^{(-)}$ interactions ought to be regarded as *stabilising bonding interactions* rather than proper intermolecular hydrogen bonds because the RING and CHAIN aggregates are not energetically stable on an absolute scale of bonding energy (i.e., in the absence of counterions). The presence of very short non-hydrogen-bridged $O\cdots O$ contacts resulting from charge compression of polyatomic anions bridged by alkali cations is also discussed.

Keywords: ab initio calculations · database analysis · deprotonated acids · hydrogen bonds · ion-molecule interactions · isomers

Introduction

Understanding the interactions that control molecular or ion recognition and self-assembly is one of the most relevant chemical problems of our time. The most important of such interactions is undoubtedly the hydrogen bond (HB) because it combines strength and directionality. The HB is defined as a stable interaction between an X–H donor and a Y acceptor, X and Y being electronegative atoms or electron-rich groups.[1] The HB interaction is generally stronger (often much stronger) than the strongest van der Waals interactions.

The packing motifs of neutral molecules carrying HB donor and acceptor groups have been extensively studied. It has been shown, inter alia, that in molecular crystals the number of HB interactions that are formed is always maximised.[2] In a top–down approach, a crystal structure can be rationalised by finding the types and number of HB motifs which, in turn, can be used to compare crystal packings. On the other hand, in a bottom–up approach to crystal packing analysis, the intermolecular HB motifs formed by the molecular building blocks are equivalent to the so-called supramolecular synthons.[3] Only those motifs that correspond to sufficiently strong and directional interactions can be observed in different crystal structures and may be exploited successfully to construct crystal architectures. Understanding the occurrence, reprodu-

[a] Prof. D. Braga, Dr. L. Maini
Department of Chemistry G. Ciamician
University of Bologna, 40126 Bologna (Italy)
E-mail: dbraga@ciam.unibo.it

[b] Prof. F. Grepioni
Department of Chemistry
University of Sassari, 07100 Sassari (Italy)
E-mail: grepioni@ssmain.uniss.it

[c] Dr. F. Mota, Dr. C. Rovira, Prof. J. J. Novoa[+]
Departament de Química Fisica, Facultat de Química
Universitat de Barcelona, 08028, Barcelona (Spain)
E-mail: novoa@qf.ub.es

[+] Queries on the theoretical part should be addressed to Professor J. J. Novoa.

  0947-6539/00/0624-4536 $ 17.50+.50/0

cibility, transferability and (possibly) the energetics of supramolecular synthons is fundamental to understanding and controlling the aggregation of molecules into crystals.

A large number of theoretical studies have been focussed on HB interactions.[4] It is now widely accepted that the HB has to be regarded as a chiefly electrostatic interaction with a variable covalent component.[5] Seminal studies have also shown that in acidic anions, as well as in chains of neutral molecules, strengthening of the interaction may result from resonance assistance when the O–H···O interactions are joined by unsaturated C=C bonds.[6] However, while HB interactions between neutral molecules and between neutral molecules and ions, including their thermochemistry,[7] have been investigated extensively, *interionic* HB interactions between ions carrying charges of the same or opposite signs have not received much attention. This is somewhat surprising, since these interactions play a fundamental role in the packing of many classes of crystalline salts, hence, in their physical and chemical properties, in the behaviour of biologically relevant molecules (e.g., amino acids and zwitterionic forms), as well as in the properties of solutions (pH, solvation, ion transport, conductivity, etc.). Furthermore, HB interactions between ions are widely employed in the engineering of sophisticated crystal superstructures.[8] The reason for this choice is simple: electrostatic forces acting between ions provide strength, while optimisation of hydrogen-bonding interactions between ions provide much of the directionality. Robustness and directionality are fundamental prerequisites for the successful design and preparation of crystalline materials with predefined solid-state properties.[9]

In approaching interionic HBs, one needs to distinguish between HB interactions involving positively charged donors and negatively charged HB acceptors (i.e., $^{(+)}$N–H···O$^{(-)}$) and the case of ions carrying the same charge (i.e., $^{(-)}$O–H···O$^{(-)}$). The former interaction represents an indisputable case of "charge-assisted" HB, since the ionic charges are "in the right place" with respect to the HB dipole.[10, 11] In the case of *homoionic* interactions the situation is more controversial because electrostatic repulsions between like charges,[11] at least in the case of small anions, can be expected to dominate over other possible attractive components associated with the $^{(-)}$O–H···O$^{(-)}$ interactions. As a consequence, the aggregation of anions through $^{(-)}$O–H···O$^{(-)}$ interactions would be energetically unstable against dissociation (in the absence of counterions). Since stability is a necessary condition for the presence of a bond,[12] we have argued[13] that the $^{(-)}$O–H···O$^{(-)}$ interactions, at least in the case of small anions such as the hydrogen oxalate, would be more appropriately described as stabilising hydrogen-bonding interactions in the presence of the dominant anion–anion electrostatic forces, rather than as conventional pairwise hydrogen bonds. This interpretation has been questioned recently.[14]

In an effort to address the problem of interanionic $^{(-)}$O–H···O$^{(-)}$ interactions in more detail (and to answer some of the questions raised by our preliminary communication[13]), we now report a comprehensive theoretical and structural study of $^{(-)}$O–H···O$^{(-)}$ interactions formed by the hydrogen carbonate (HCO_3^-), the hydrogen oxalate ($HC_2O_4^-$),[15] the hydrogen squarate ($HC_4O_4^-$) and the hydrogen croconate ($HC_5O_5^-$) anions, hereafter collectively indicated as HA^-. In addition, we report the preparation and structural characterisation of the novel hydrogen croconate salts $NaHC_5O_5 \cdot H_2O$ and $CsHC_5O_5$ and the structural redetermination of $RbHC_5O_5$.[16]

By means of two complementary approaches, namely ab initio computational methods,[17] and investigation of the Cambridge Structural Database (CSD) and of the Inorganic Crystal Structure Database (ICSD),[18] we will address the following questions:

1) Are there preferential packing motifs for small HA^- anions connected by $^{(-)}$O–H···O$^{(-)}$ interactions in the solid state?
2) Can we estimate, and possibly rationalise, the difference in energy between these motifs?
3) Can we gain insight, from the results of a rigorous ab initio computational approach, into the factors responsible for the cohesion of crystalline salts formed by anions connected by $^{(-)}$O–H···O$^{(-)}$ interactions?
4) Can we discriminate between the components (electrostatic, exchange–repulsion, polarisation, charge transfer and dispersion) of the $^{(-)}$O–H···O$^{(-)}$ interaction energy and observe similarities and differences between these interactions and neutral O–H···O hydrogen bonds?
5) Can we evaluate the effect of the medium (i.e., the solution and crystalline solid) on the $^{(-)}$O–H···O$^{(-)}$ interaction?
6) Can we provide further experimental information on the preferential packing motifs adopted by HA^- anions in the solid state?

To answer these questions database searches have been carried out for all HA^- anions listed above. Since the structures of very few hydrogen croconates are known, they have not been considered in the statistical analysis. The theoretical approach has been focussed on the interaction between hydrogen carbonate anions such as $HCO_3^-\cdots HCO_3^-$, because the size of the anions makes them amenable to full ab initio characterisation. The energy of the interaction has been broken down into its constituent components in order to analyse the relative contribution of all its components. The potential energy curves, computed for the approach of OH^-, Cl^- and HCO_3^- anions from infinity to interaction distance, have been compared. The effect of a cage of solvent molecules on the aggregation of hydrogen oxalate anions in solution has been evaluated. Similarly, the effect, in the crystal, of the Madelung field on the polarisation of the ions involved in interanionic $^{(-)}$O–H···O$^{(-)}$ interactions has been investigated. Finally, the ring and chain motifs present in the hydrogen croconate salts $CsHC_5O_5$ and $RbHC_5O_5$[16] have also been examined computationally.

Results and Discussion

Occurrence of the ring and chain motifs in ionic crystals: Neutral carboxylic and polycarboxylic acids can either form ring (RING hereafter) or chain (CHAIN hereafter) motifs in their crystals (see Scheme 1). These latter motifs are also known as *catemers*.[19]

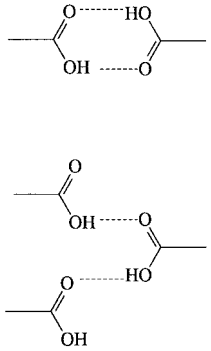

Scheme 1. The RING (top) and CHAIN (bottom) motifs present in crystals of neutral carboxylic acids.

Pioneering studies of the packing of organic carboxylic acids were carried out by Leiserowitz and Schmidt, who also investigated the O–H···O bonding by atom–atom potential energy methods.[19c] Ab initio calculations have been carried out by Dannenberg et al.,[20] while, more recently, molecular dynamics calculations, based on atom–atom potentials, have been carried out on acetic and tetrolic acids by Gavezzotti[21] with the aim of understanding molecular aggregation and crystal nucleation processes.

In crystals of neutral polycarboxylic acids the CHAIN motif is not very frequent. A recent CSD survey has shown that the RING motif is observed in 95% of the structures of neutral carboxylic and polycarboxylic molecules.[22] A notable exception is acetic acid which forms the CHAIN motif in the solid state,[23] although it has been demonstrated by theoretical calculations that the acetic acid RING is favoured over CHAIN by approximately 3 kcal mol^{-1}.[24a] These differences were explained by invoking the contribution of other weak intermolecular interactions in the solid state with respect to the structure of the isolated dimers in a vacuum.[24b] Oxalic acid, on the other hand, is known to form both types of patterns in different polymorphs.[25] Similar situations are known for other acids, including several organometallic complexes.[26]

On passing from neutral to monodeprotonated acids the HB capacity evidently changes. While no homoionic HB is possible between deprotonated monocarboxylic acids, such as the acetate anion, the possibility of RING–CHAIN isomerism persists in the case of anions derived from polyprotic acids, such as the hydrogen oxalate and hydrogen carbonate anions, as well as in the case of hydrogen keto–enolate anions, such as hydrogen squarate and hydrogen croconate. Scheme 2 shows the model RING and CHAIN motifs in the cases of a) the smallest HA^- anion (i.e., the hydrogen carbonate anion) and b) the hydrogen oxalate anion. For the purpose of this paper, alcohols are not considered.

The results of the CSD and ICSD searches of the RING and CHAIN motifs in crystalline salts that contain HB interacting hydrogen carbonates (HCO_3^-), hydrogen oxalates ($HC_2O_4^-$) and hydrogen squarates ($HC_4O_4^-$) anions are summarised in Table 1. The three types of HA^- anions appear to behave in a very different manner with respect to the choice of HB motif. Although the number of observations is not large and care should be taken to avoid an overconfident use of the statistical values, the following tendencies are observed:

1) Hydrogen carbonates preferentially form RINGs; the CHAIN pattern has been observed (as yet) only in crystalline $NaHCO_3$ (see below).[27] A space-filling representation of the RING and CHAIN motifs in $KHCO_3$ and $NaHCO_3$ is shown in Figure 1.
2) In contrast to hydrogen carbonates, hydrogen oxalates only form CHAINs in the solid state [i.e., no RING is (as yet) known]. There are also 11 hydrogen oxalate salts in which no direct interanion HB interactions are observed. The O···O distances in the CHAIN systems fall in the range 2.435–2.616 Å.
3) Hydrogen squarates form both RINGs and CHAINs. Although the mean O···O distances in hydrogen squarate RING pattern is shorter than in the more populated CHAIN systems, the spread is very different: while O···O distances in hydrogen squarate CHAIN are as long as 2.620 Å, the longest distance in RINGs is 2.517 Å.
4) In the hydrogen squarate CHAINs and RINGs the O···O separations are significantly shorter, both in distance range and in mean value, than in hydrogen carbonates.

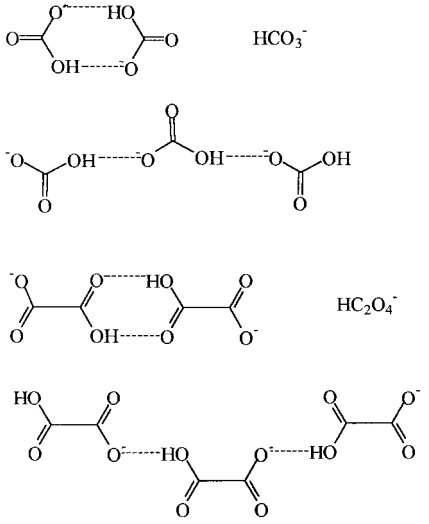

Scheme 2. RING and CHAIN motifs between hydrogen carbonate (top) and hydrogen oxalate anions (bottom).

Theoretical analysis of the interanionic $^{(-)}$O–H···O$^{(-)}$ interaction in the vacuum: In this section we will investigate the nature of the $^{(-)}$O–H···O$^{(-)}$ short contacts in a rigorous form.

Table 1. Distances ranges, mean values (esd), lowest 10% quantiles, and number of observations for the hydrogen carbonate HCO_3^-, the hydrogen oxalate $HC_2O_4^-$ and the hydrogen squarate $HC_4O_4^-$ anions [all distances in Å].

	RINGS				CHAINS			
	Distance range	Mean value (esd)	Lowest 10% quantiles	Number of observations	Distance range	mean value (esd)	Lowest 10% quantiles	Number of observations
HCO_3^-	2.545–2.641	2.593(32)	2.545	12	2.611[b]			
$HC_2O_4^-$[c]	–	–	–	–	2.435–2.616	2.533(76)	2.461[a]	35
$HC_4O_4^-$	2.476- 2.517	2.500(17)	2.476	5	2.409–2.620	2.524(64)	2.510	19

[a] From ref. [15]. [b] Only one case of CHAIN, $NaHCO_3$. [c] No RING observed; 11 hydrogen oxalate salts do not show interanion interactions.

0947-6539/00/0624-4538 $ 17.50+.50/0 *Chem. Eur. J.* **2000**, *6*, No. 24

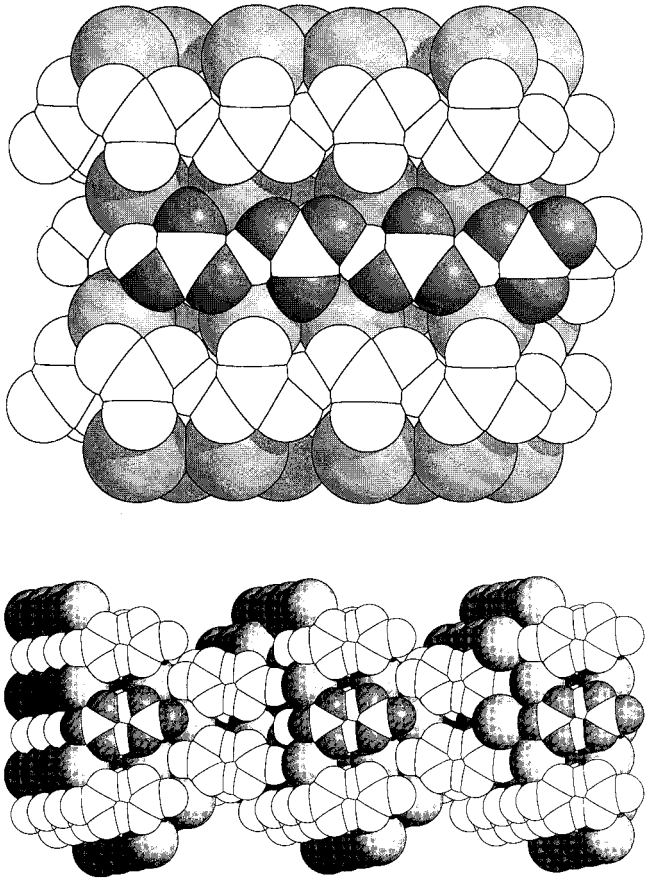

Figure 1. Space-filling representation of the ion packing in $NaHCO_3$ (top) and $KHCO_3$ (bottom); note the CHAIN and RING motifs, respectively.

The ab initio methods of choice provide an insight on all the components of the interaction energy, not only a few terms of its electrostatic component, as are obtained by simply modelling the interaction energy in terms of the atomic charges on the atoms. The present analysis, therefore, updates the first-principle qualitative approach applied to the hydrogen oxalate anion.[13] That preliminary study was based on an analysis of the electrostatic potential energy maps of the isolated (gas phase) ion, and, though qualitatively superior to the point-charge model, could not deal with the dispersion, charge transfer or exchange–repulsion terms known to be non-negligible in the energetic evaluation of HB interactions.[4, 5, 11b]

In order to appreciate the attractive or repulsive nature of the $^{(-)}O{-}H\cdots O^{(-)}$ contacts found in the CHAIN and RING motifs, we investigate the anion HCO_3^-, which is known to present these two motifs in crystalline $NaHCO_3$ and $KHCO_3$, respectively. Also, the size of the anion permits a thorough quantum chemical ab initio analysis, including second-order Møller–Plesset (MP2) computations.

In a simplistic first approach, two HCO_3^- ions moving close together may be expected to repel each other as if they were two spherical anions such as Cl^-. The ab initio computation, however, shows that this view holds true only when the anions are far apart. At large separation, the HCO_3^- anions create a field of the type $^1/_r$, behaving as spherical ions. However, on decreasing the interanion distance, the local dipole–charge and dipole–dipole terms, which have a $^1/_r{}^n$ ($n>1$) dependence, affect the strength of the interanion interaction. We have seen in the case of $HC_2O_4^-$ anions[11b] that the overall effect of these terms is not large enough to make the CHAIN interaction stable at the geometry of the KHC_2O_4 crystal. In that work, however, we did not investigate the nature of the interaction in detail, neither did we compare the energetics of the CHAIN and RING motifs.

These aspects will be dealt with in the case of the HCO_3^-–HCO_3^- interactions in the following sections.

Energy decomposition of the $HCO_3^-\cdots HCO_3^-$ interactions at the crystal geometry: Insight into the nature of the $^{(-)}O{-}H\cdots O^{(-)}$ interaction in the CHAIN and RING motifs can be obtained by performing an energy decomposition of the intermolecular interaction at the geometry adopted by the HCO_3^- anions in the $NaHCO_3$ and $KHCO_3$ crystals. The energy components for these two dimers, computed by using the intermolecular perturbation theory (IMPT) scheme,[28] are reported in Table 2. This method provides a rigorous ab initio breakdown of the total interaction energy (E_{tot}) into physically meaningful terms: electrostatic (E_{el}), exchange–repulsion (E_{er}), polarisation (E_{pol}), charge transfer (E_{ct}) and dispersion (E_{disp}) energies. The method is free from the unwanted basis-set superposition error (BSSE) present in other methods due to the use of truncated basis sets. Furthermore, the total interaction energy provided by this method for the HCO_3^- anion is nearly identical to that computed using the second-order Møller–Plesset (MP2) method, once extended basis sets are used and the BSSE is corrected (see Experimental Section).

Table 2. Energy break down [kcal mol^{-1}] for the HCO_3^- CHAIN and RING motifs.

	CHAIN	RING
E_{el}	42.6	−4.6
E_{er}	31.8	55.6
E_{pol}	−7.3	−10.3
E_{ct}	−5.4	−8.9
E_{disp}	−10.9	−24.2
E_{tot}	50.9	7.6

The energy terms for the RING and CHAIN HCO_3^- dimers have been computed at the same level of accuracy as those reported previously for the OH^- and $HC_2O_4^-$ dimers,[11b] that is, by using the 6–31+G(2d,p) basis set. The following facts can be noted:

1) Both dimers have positive interaction energies, that is, their energy lies above the energy of two isolated HCO_3^- anions separated infinitely.
2) The RING is more stable than the CHAIN motif by 43.3 kcal mol^{-1}.
3) The IMPT energy component analysis shows that the main reason for the increased stability of the RING motif is the much higher stability of the electrostatic component, more stable than in the CHAIN motif by 47.2 kcal mol^{-1}.
4) On the other hand, the variation of the exchange–repulsion term that disfavours RING over CHAIN is compen-

sated by an opposite variation of the dispersion, polarisation and charge transfer terms.

It is also interesting to note that the value of the electrostatic term in the HCO_3^- CHAIN (42.6 kcal mol^{-1}) is intermediate between those previously obtained for the OH^- (90.5 kcal mol^{-1}) and $HC_2O_4^-$ dimers (16.7 kcal mol^{-1})[11a] with corresponding $r(H\cdots O)$ bond lengths of 1.957 and 1.482 Å (as in the water dimer and in the KHC_2O_4 crystal, respectively).[11b] This comparison allows one to see that the strong electrostatic repulsion found in the OH^- dimer corresponds to the largest separation, which is the opposite of what one would expect from a simple $^1/_r$ dependence of the electrostatic interaction. This fact can only be explained by noticing that the repulsion is mostly due to the amount of the negative net charge localised on the OH group involved in the short O–H···O contact. The near -1 charge on the OH^- group in the $OH^-\cdots OH^-$ dimer becomes -0.34 and $-0.05\,e^-$ in the HCO_3^- and $HC_2O_4^-$ CHAIN dimers, respectively, while the charge located on the O acceptor atom varies much less (-1.13, -0.92 and , -0.83 e$^-$ in the OH^-, HCO_3^- CHAIN and $HC_2O_4^-$ CHAIN dimers, respectively; Hartree–Fock charges). Consequently, delocalisation of the net negative charge of the anion donor over a large number of atoms and *away from the −OH group* decreases the electrostatic repulsion.[29] This is in keeping with our database analysis of the geometric features of −COOH and $-COO^{(-)}$ groups in crystals of neutral, ionic and zwitterionic forms of carboxylic acids and carboxylate anions; this provides clear evidence that, upon deprotonation, the negative charge remains mostly confined on the $-COO^{(-)}$ groups, irrespective of the neutral or ionic nature of the acid and of the size of the systems.[15]

MP2 interaction energies and a comparison of the potential energy curves: In order to gain further insight into the effect of the H···O short contact on the $^{(-)}$O–H···O$^{(-)}$ interaction we have compared the *shape* of the CHAIN and RING potential energy curves calculated for the HCO_3^- dimer with that obtained for the hypothetical $Cl^-\cdots Cl^-$ and $OH^-\cdots OH^-$ dimers. This analysis is expected to yield useful information on the factors controlling the relative stability of the two motifs. Figure 2 shows the MP2 interaction energy computed by using the 6–31++G(d) basis set for the $Cl^-\cdots Cl^-$, the $OH^-\cdots OH^-$ and both the CHAIN and RING $HCO_3^-\cdots HCO_3^-$ dimers, as a function of $Cl^-\cdots Cl^-$ or H···O distances, as appropriate. The internal geometry and the orientation of the HCO_3^- anions were kept constant in computing these curves. The graphs clearly show that, although the four curves are repulsive, at short distances the HCO_3^- RING and CHAIN dimers are more stable than the Cl^- and OH^- dimers, while at large distances all dimers have a similar interaction energy. As we shall discuss further below, the increased stability accompanying the decrease in the inter-anion H···O distance, *can be attributed to the appearance of an attractive component accompanying the delocalisation of the net negative charge away from the OH group.* As a consequence of this stabilising interaction, there is an inflection in the potential energy curve of the HCO_3^- CHAIN, and a metastable minimum in the curve of the HCO_3^- RING. These features are diagnostic of the existence of a stabilising interaction, which is more pronounced in the RING than in the CHAIN dimer. On the other hand, if the negative charge is localised on an atom or pair of atoms (as in the case of the Cl^- and OH^-anions), the interaction is dominated by the repulsive components at all distances.

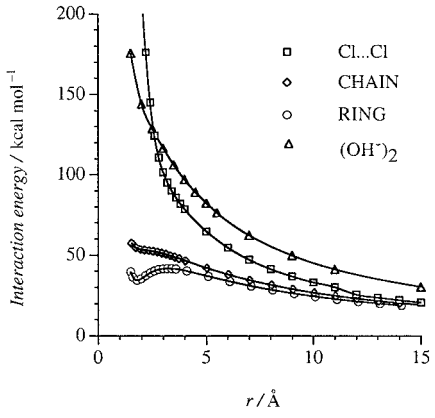

Figure 2. The MP2 interaction energy computed using the 6–31++G(d) basis set for the Cl^-, OH^-, HCO_3^- CHAIN and HCO_3^- RING motifs (see Scheme 2 top), as a function of the Cl···Cl and H···O distances, respectively.

Hence, the presence of other groups bound to the OH donor is necessary to achieve charge delocalisation away from the OH group and to observe the increase of the stabilising interaction between the functional groups.

It is also worth noting that the relatively small energy needed to form the metastable RING dimer from two separate anions is not inconsistent with the presence of RING dimers in solution of HA^- anions, for which additional stabilisation may arise from solvation effects. Formation of long-living RING dimers detectable by spectroscopic techniques should then be a reasonable hypothesis. This point will be addressed in more detail below.

IMPT calculations of the variation of the interaction energy components with distance: A better understanding of the interaction energy curves can be obtained by examining the change of the energy components (Figure 3) resulting from the IMPT study for the RING and CHAIN HCO_3^- dimers and for the OH^- dimer. Since the IMPT procedure does not properly reproduce the shape of the MP2 curve at $r(H\cdots O)$ distances shorter than 1.5 Å, these parts of the curves have not been included in the graphs. At large distances the dominating component in both RING and CHAIN curves is the electrostatic term, which is repulsive in character. At distances shorter than 2.5 Å the repulsive component decreases, and the decrease is particularly pronounced in the case of the RING motif. This decrease of the electrostatic repulsion is, however, accompanied by an increase of the repulsive exchange–repulsion term, while all the attractive components (dispersion, polarisation and charge transfer) increase their stabilising contribution as the distance is shortened. The shape of the variation of the energy components is the same for the RING and CHAIN motifs, with the notable difference that the electrostatic curve is shifted towards lower energies in the RING case. This fact not only reflects the presence of two O–H···O contacts in the RING motif (see below), but also

  0947-6539/00/0624-4540 $ 17.50+.50/0 *Chem. Eur. J.* **2000**, *6*, No. 24

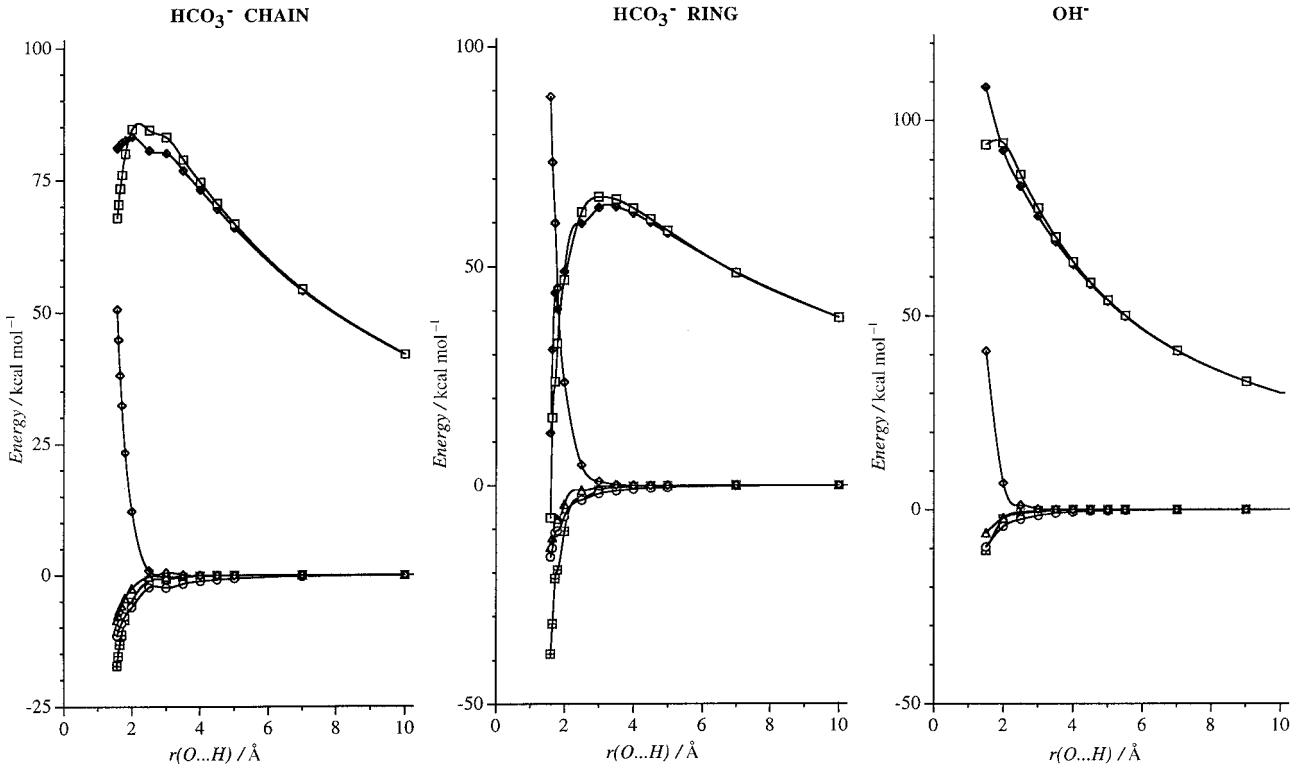

Figure 3. IMPT computation of the components of the interaction energy in the HCO_3^- RING and CHAIN motifs as a function of the $r(H\cdots O)$ distance. $\square = E_{el}$, $\bigcirc = E_{pol}$, $\boxplus = E_{disp}$, $\diamond = E_{er}$, $\triangle = E_{ct}$, $\blacklozenge = E_{tot}$.

that the electrostatic component is the one responsible for the change in character of the interaction. Figure 3 also shows that in all cases the electrostatic component is nearly identical to the total interaction energy down to $H\cdots O$ separation of 2 Å.

In order to simulate the effect of lengthening the CHAIN motif, the IMPT analysis was carried out on the model system shown in Scheme 3. This can be used to evaluate the impact of

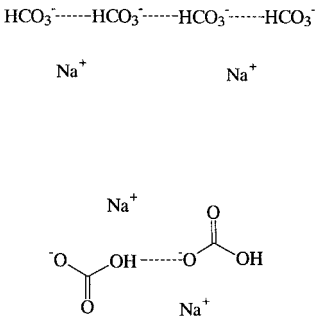

Scheme 3. The "long" CHAIN system used to evaluate the effect of neighbours on the $HCO_3^-\cdots HCO_3^-$ interaction.

the nearest neighbours on the strength and variation of the energy components in a longer $HCO_3^-\cdots HCO_3^-\cdots HCO_3^-$ chain. At the crystal geometry, the electrostatic component is repulsive by 19.67 kcal mol^{-1}, and the total energy by 25.23 kcal mol^{-1}, lower than when only two HCO_3^- anions are considered, as expected. This is, however, a lower limit value: given the $^1/_r$ dependence of the charge–charge electrostatic term, repulsions and attractions between non-adjacent ions are felt also at long distance. Indeed, when all $HCO_3^-\cdots HCO_3^-$, $HCO_3^-\cdots Na^+$ and $Na^+\cdots Na^+$ terms are considered, the interanion repulsion in the central $HCO_3^-\cdots HCO_3^-$ increases again. The role of the cations will be discussed in more detail later.

The nature of the $^{(-)}O{-}H\cdots O^{(-)}$ interactions found in the RING and CHAIN motifs: In order to understand the reasons for the change of slope with the distance of the electrostatic energy curves of the RING and CHAIN HCO_3^- dimers, the electrostatic component has been separated into interaction terms associated with the following fragments: the OH group, the O_a acceptor atom of the $^{(-)}O{-}H\cdots O^{(-)}$ shortest contact, and the remaining CO group (Scheme 4). Each term was computed by using a distributed multipole expansion of the electrostatic energy up to the quadrupole term (see Experimental Section). There are nine different interaction terms in the CHAIN dimer and only six in the RING dimer, due to the higher symmetry of the latter. The partitioning yields both repulsive and attractive components, which are plotted as a function of interanion distance in Figure 4. One can note that:

1) There are two components in the RING motif which are always attractive over the whole curve, namely the $CO\cdots O_a$ and the $OH\cdots CO$ interactions (see Scheme 4).
2) There are two interactions of this type and their sum is practically compensated by the three repulsive terms between the like fragments, namely the $OH\cdots OH$, $CO\cdots CO$ and $O_a\cdots O_a$ interactions.
3) Importantly, there is also an interaction which is repulsive at large distances, *but* becomes attractive at short distances; this is the $O{-}H\cdots O_a$ interaction. There are two

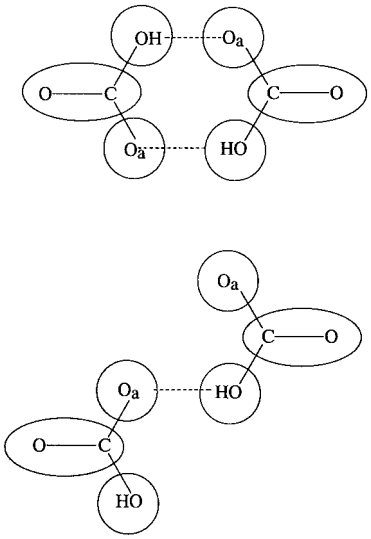

Scheme 4. Atomic labelling for the energy plot in Figure 4.

such interactions in the RING motif and these vary from 20 kcal mol^{-1} at 3 Å to -10 kcal mol^{-1} at 1.25 Å, and have a similar variation in the CHAIN motif.

4) Such a change in the dominant energetic component is due to a *change in the nature of the O–H $\cdots$ O$_a$ interaction*: at large distances the interaction is dominated by the interaction between two negative charges (or a negatively charged dipole and a negative charge), but at short distances it becomes dominated by the interaction between a partly negatively charged O$_a$ atom and the H end of the O–H dipole, which bears a positive charge. Clearly, this dominant component at very short separation is present twice in the RING with respect to the CHAIN motif.
5) The situation, although slightly more complex due to the lack of symmetry, is similar in the CHAIN motif, although here only one O–H $\cdots$ O$_a$ term becomes strongly attractive as the anions get closer.
6) We have verified that the previous trends are not found in the *neutral* RING and CHAIN dimers, that is, they are specific to the interanionic systems studied here.

It is interesting to note that, in both RING and CHAIN motifs, the electrostatic interaction between the OH groups is repulsive at all distances. The O–H $\cdots$ O$_a$ electrostatic term at short separation, and the OH $\cdots$ CO and O$_a^-$ $\cdots$ CO terms in the whole distance range are responsible for the higher stability of the $HCO_3^- \cdots HCO_3^-$ system with respect to the $Cl^- \cdots Cl^-$ and $OH^- \cdots OH^-$ fragments as shown by the respective potential energy curves. It should also be noted that if the $HCO_3^- \cdots HCO_3^-$ interaction is considered as being composed of an O–H $\cdots$ O$_a$ hydrogen bond to which the interactions created by the remaining parts of the two HCO_3^- molecules are added, the calculations show *that the O–H $\cdots$ O$_a$ interaction is attractive only at very short H $\cdots$ O distances* (less than 1.50 Å), because at larger distances the interaction is nothing other than that between a negatively charged $OH^{\delta-}$ fragment and a negatively charged $O^{\delta-}$ atom. Since this interaction is repulsive it would prevent formation, in vacuum, of HCO_3^- dimers or higher aggregates.

Since all previous values have been obtained for CHAIN and RING dimers in vacuum, one may object that the conclusions do not extend to condensed phases. We will demonstrate below that this is not the case with three sets of computational evaluations:

1) by computing the stability of the dimers in solution,
2) by studying the electronic properties of the dimers in their crystals and
3) by carrying out computations on small aggregates in which more cations and anions are attached to the HCO_3^- dimer in the same positions as that found in the crystal.

We anticipate that these experiments will show that the electron distribution evaluated in these three conditions does not differ very significantly from the vacuum and that the net effect of the media is to

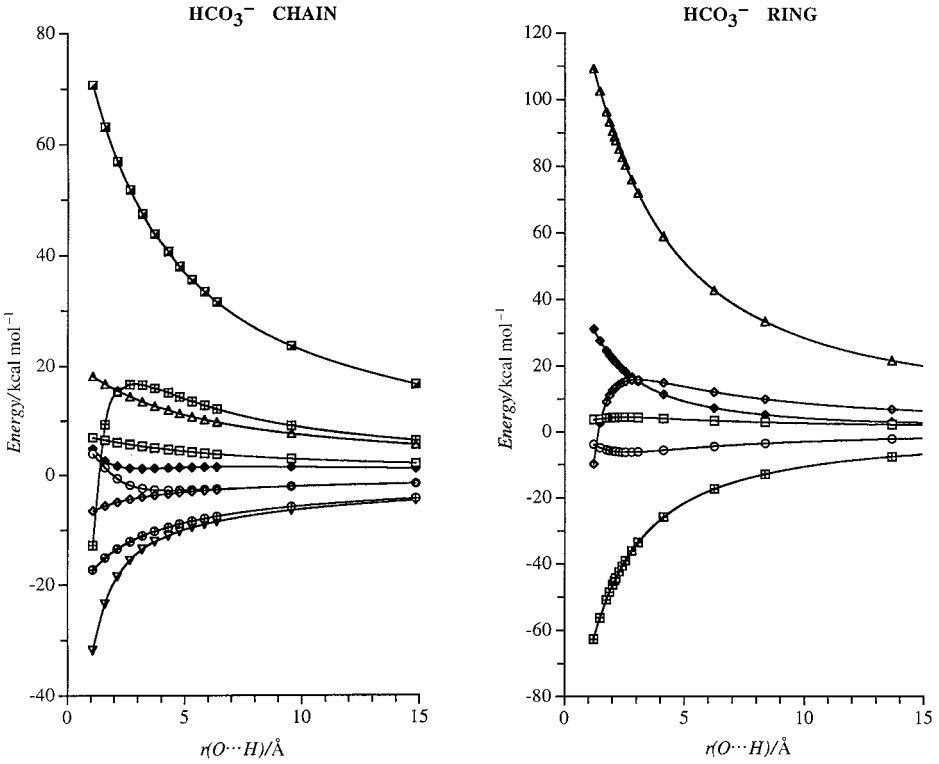

Figure 4. Partitioning of the electrostatic interaction between HCO_3^- anions into components associated with the functional groups of the OH group, the O$_a$ acceptor atom of the O–H $\cdots$ O shortest contact and the remaining CO$_b$ group. Left: □ = OH $\cdots$ OH, ◇ = CO $\cdots$ OH, ○ = OH $\cdots$ CO, △ = O$_a$ $\cdots$ OH, ⊞ = OH $\cdots$ O$_a$, ◆ = CO $\cdots$ CO, ⊕ = O$_a$ $\cdots$ CO, ▽ = CO $\cdots$ O$_a$, ◪ = O$_a$ $\cdots$ O$_a$. Right: □ = OH $\cdots$ OH, ◇ = OH $\cdots$ O, ○ = OH $\cdots$ CO, △ = CO $\cdots$ CO, ⊞ = O $\cdots$ CO, ◆ = O $\cdots$ O.

0947-6539/00/0624-4542 $ 17.50+.50/0 *Chem. Eur. J.* **2000**, *6*, No. 24

increase the stability of both the CHAIN and RING motifs. However, while the slightly metastable RING motif will be stabilised, the CHAIN motif will remain unstable with respect to dissociation in the absence of counterions.

Behaviour in solution—ab initio molecular dynamics study of the $HC_2O_4^- \cdots HC_2O_4^-$ dimers by using the Carr–Parrinello method: The first step is the study of the aggregate lifetimes in solution. Of course, the solvent used in the simulation cannot be water because of its hydrogen-bonding capacity; the choice of solvent also limits the choice of the anion. Therefore we have chosen to study the stability of a cluster formed by hydrogen oxalate anions in chloroform solution, because salts of this anion with relatively large organic cations are known to be soluble in chloroform.

The model cluster $\{(HC_2O_4^-)_2 \cdots (CH_3Cl)_{14}\}$ is obtained by distributing 14 molecules of CH_3Cl around the $HC_2O_4^-$ RING and CHAIN dimers, thus forming an equal density surface which simulates the dimer first solvation shell. The $\{(HC_2O_4^-)_2 \cdots (CH_3Cl)_{14}\}$ cluster is then subjected to a full geometry optimisation at the HF/6 – 31 + G level leading to two different results: i) when the $(HC_2O_4^-)_2$ unit is a RING, a minimum is found in which the geometry of the two anions is similar to that found in the gas phase and ii) when the $(HC_2O_4^-)_2$ unit is a CHAIN, the optimised structure shows the presence of two $HC_2O_4^-$ anions separated by chloroform molecules (i.e., the CHAIN dimer dissociates).

The optimised $\{(HC_2O_4^-)_2 \cdots (CH_3Cl)_{14}\}$ cluster containing a RING dimer, together with the optimised unsolvated CHAIN and RING dimers for comparison, were then taken as the starting point in an ab initio molecular dynamics study based on the Carr–Parrinello method.[30] The variation of the $^{(-)}O–H \cdots O^{(-)}$ distance for the three systems against time is plotted in Figure 5. Clearly, the RING $(HC_2O_4^-)_2$ dimer is stable after 1.5 picoseconds and shows no tendency to dissociate or change its structure (see the periodic change in the two O–H···O distances in Figure 5). The solvated RING shows the same trend as the gas phase RING dimer and only periodic variation of the O–H···O distances have been observed in a 0.6 picosecond timescale. Although this time interval is short, it is long enough to show the behaviour of the systems with time. Our results suggest that the solvated RING dimers, once formed, could possess a long enough lifetime as to be observable with techniques which are sensitive to short lifetimes (e.g., NMR spectroscopy). We did not carry out a similar ab initio dynamics on the CHAIN dimer, as we did not find a minimum in which the $(HC_2O_4^-)_2$ was preserved when optimising the structure of the CHAIN $\{(HC_2O_4^-)_2 \cdots (CH_3Cl)_{14}\}$ cluster at the Hartree–Fock/6 – 31 + G level.

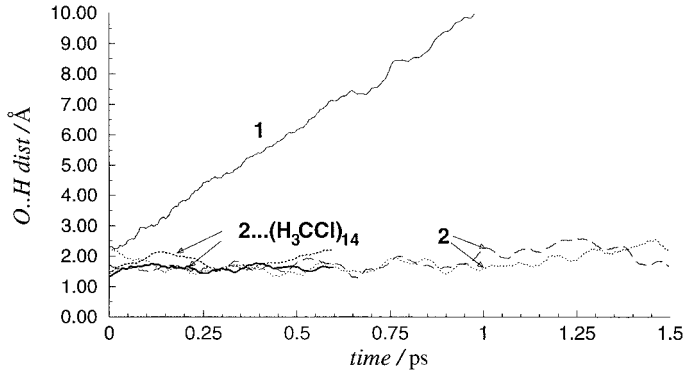

Figure 5. The variation of the O–H···O distance and the dynamics for the isolated CHAIN (1) and RING (2) dimers and for the cluster $(HC_2O_4^-)_2 \cdots (CH_3Cl)_{14}$ containing a RING. Note the rapid dissociation of the isolated CHAIN dimer.

The $HCO_3^- \cdots HCO_3^-$ and $HC_2O_4^- \cdots HC_2O_4^-$ RING and CHAIN dimers in the solid state: The main difference felt by HA^- anion dimers on passing from the vacuum to the crystal arises from the Madelung field created by the surrounding anions and cations. The surrounding charges are likely to cause a polarisation of the electron distribution on the anion dimers in the crystal with respect to the isolated dimer.

Such polarisation has been evaluated in the cases of the CHAINs present in KHC_2O_4 and $NaHCO_3$ by computing the (Mulliken) atomic charges of i) an isolated anion, ii) an isolated dimer, iii) an isolated dimer surrounded by its first and second neighbour anions and iv) the same dimer within the observed crystal structure. In this last case the atomic charges provided by CRYSTAL[32] were used.

In the case of the $HC_2O_4^-$ anion, the charges on the O–H···O atoms are i) – 0.62, 0.50 and – 0.83 e^- in the isolated anion, ii) – 0.60, 0.55 and – 0.74 e^- in the isolated dimer and iii) – 0.61, 0.56 and – 0.76 e^- in a dimer surrounded on both sides by two other dimers. The CRYSTAL calculations afford charges of – 0.72, 0.49 and – 0.77 e^- for an isolated dimer and charges of – 0.75, 0.34 and – 0.77 e^- for the observed crystal.

The same trend is found when analysing the $-COO^{(-)}$ acceptor group. When computed with CRYSTAL at the geometry observed in crystalline KHC_2O_4 the charges are C 0.77 e^-, O(acceptor) – 0.83 e^- and O(no acceptor) – 0.77 e^-. The Mulliken charge model, though simple, shows two important facts: i) the two oxygen atoms on the acceptor carry almost the same charge, indicating extensive delocalisation over the two O atoms of the –COO group and ii) the overall charge on the group is close to – 1. This is in agreement with the database analysis of the geometry of –COOH and $-COO^{(-)}$ groups in hydrogen oxoacid anions and zwitterions.[15] Interestingly the fact that the two C–O bond lengths within the group are not the same [average C–O(acceptor) and C–O(no acceptor) bond lengths in hydrogen oxalate salts 1.256(2) versus 1.234(2) Å, respectively] does not affect the electronic distribution of the molecule: when the isolated anion is fully optimised in vacuum the charges on the $-COO^{(-)}$ group do not change with respect to the crystal geometry, whereas the two C–O bond lengths become equal (1.222 Å).

Therefore, the difference in the two C–O bond lengths has to come from the interactions in the crystal. The slightly higher value of the charge in the O(acceptor) atom of the $-COO^{(-)}$ group is probably caused by the polarisation induced by the positive charge of the H atom of the donor group (+ 0.50).

When the charges discussed above are employed the interanion electrostatic energy in the CHAIN motif remains repulsive. The charge–charge electrostatic energy is

55.80 kcal mol^{-1} if the CRYSTAL charges are used, while it is 62.71 kcal mol^{-1} when computed with the isolated monomer atomic charges (the latter value has to be compared with a repulsion of 66.62 kcal mol^{-1} computed with the distributed multipole analysis (DMA) values). Thus the interaction between anions in CHAINs on passing from the vacuum to the crystal remains strongly repulsive. Hence, the overall stability of the KHC_2O_4 crystal, as well as that of $NaHCO_3$ which also contains anionic chains, cannot be attributed to the contribution of the $^{(-)}O{-}H\cdots O^{(-)}$ interactions, but to the compensation created by the attractive cation – anion attractions with respect to the anion – anion and cation – cation repulsions, in agreement with what was previously reported.[11, 13]

The situation is different in the case of the RING motif (e.g., $KHCO_3$). When the CRYSTAL charges are used the charge-charge repulsion decreases to 15.90 kcal mol^{-1}, compared with the 47.03 kcal mol^{-1} value found by using the isolated charges of each monomer, or to 49.89 kcal mol^{-1} calculated from the DMA multipole expansion. Therefore, the polarisation induced by the Madelung field (accounted for accurately by means of CRYSTAL computations) in the case of the RING dimer is sufficient to lower the repulsion by 31 kcal mol^{-1} with respect to that in vacuum. Since the electrostatic component is responsible for the changes of the total interaction energy (see above) the gain in stability of the RING dimer in the presence of the Madelung field is sufficient to change its nature from slightly unstable in the gas phase to stable in the crystal.

The role of the cations and the covalent component of the $^{(-)}O{-}H\cdots O^{(-)}$ interaction: So far, our results have shown that the RING motif should be considered as the most stable form of aggregation of HA^- anions in their salts. The RING motif is metastable in gas phase, but its lifetime in solution is sufficiently long to be considered as a new supramolecular entity. Furthermore, it requires little or no energy to become stable in the solid state under the effect of the Madelung field. RINGs are observed in the crystal packing of $KHCO_3$ and of all other hydrogen carbonates (except $NaHCO_3$). Figure 1 (bottom) shows how the RING dimers form ribbons separated by $(K^+)_2$ units in crystalline $KHCO_3$. These ribbons pile up in such a way that consecutive dimers are displaced with respect to its neighbour, and two cations are placed between the dimers. Indeed, in terms of anionic superstructure the crystal would be more adequately described as "$K_2[(HCO_3)_2]$".

The computations have also shown that stability (or metastability) is not attained by anions in CHAIN dimers, even though the CHAIN motif is observed in a large number of crystalline salts (see Table 1) including $NaHCO_3$. Clearly, the role of the cations in determining the formation of a stable crystal needs to be investigated.

To this end a geometry optimisation at the HF/6 – 31+G(d) or B3LYP/6 – 31+G(d) level of a $Na_2(HCO_3)_2$ tetraionic unit as present in the $NaHCO_3$ crystal has been carried out. The aggregate is energetically stable against its dissociation into two Na^+ cations and two HCO_3^- anions, even though in the optimised structure the $H\cdots O$ bond length is longer (2.5 Å) than in the crystal (1.56(2) Å). Furthermore, all vibrational frequencies are positive, hence the tetraionic unit represents a true energy minimum. Evidently, when the two cations are removed, the HCO_3^- CHAIN dissociates, that is, the $Na_2(HCO_3)_2$ teraionic unit is only stable due to the presence of the cations. The situation does not change when the effect of the Madelung field is simulated by local point charges at fixed positions around the tetraionic unit mimicking the field generated by the ions in the $NaHCO_3$ crystal.

An analysis of the properties of the $Na_2(HCO_3)_2$ tetraionic unit shows that, despite the fact that the $HCO_3^-\cdots HCO_3^-$ interaction is not energetically stable, *it has some of the properties that one would take as diagnostic of the presence of an $O{-}H\cdots O$ hydrogen bond*. For instance, there is a charge transfer from the proton-donor anion to the proton-acceptor anion in the isolated dimer, which amounts to 0.06 e$^-$, a value similar to that found in dimers of neutral molecules placed in the same CHAIN conformation. This charge transfer is due to the similarity between the orbital interactions diagrams of the neutral – neutral and of the anion – anion dimers. In both cases, it is a three-centre two-electron problem, involving the doubly occupied orbital of the proton-acceptor fragment and the empty orbital of the proton-donor fragment (see Scheme 5), regardless of the fact that the neutral dimer is stable against dissociation whilst the anionic one is not. The only difference between the two diagrams is the shift towards less stable energies of the orbitals of the HCO_3^- anion relative to those of the H_2CO_3 neutral molecule. Importantly, *in both cases* there is a new interfragment orbital formed by the combination of the orbitals belonging to the donor and acceptor fragments, the former participating with a larger weight. Thanks to this difference it is possible to transfer charge from the acceptor to the donor. The amount of charge transferred only depends on the distance between the two fragments. Therefore, if two HCO_3^- units are held together at short distance (by the cation – anion attractions), the orbitals combine forming an interfragment orbital delocalised over the two fragments (see Figure 6) which is responsible for the charge transfer (if the interaction between the proton donor and acceptor units were purely ionic in nature, the orbitals of the fragment would not combine).

Another important point is that the amount of charge delocalisation, for a given proton donor and acceptor unit, *depends only on the distance between these units and not on the cations employed in the tetraionic unit*. This assertion has been demonstrated by carrying out ab initio computations on tetraionic units obtained by substituting K^+ and $N(CH_3)_4^+$ cations for Na^+ showing that, upon optimisation, the $H\cdots O$ distance for a given anion does not change much ($<10\,\%$) with the cation. We have also observed that the amount of charge transfer between hydrogen oxalate anions in the model tetraionic units $X_2(HC_2O_4)$ [$X = Na^+$, $N(CH_3)_4^+$] is comparable with that found in $X_2(HCO_3)$ aggregates [$X = Na^+$, $N(CH_3)_4^+$].

We would like to mention here that the existence of combination between the molecular orbitals of water molecules has been taken as a sign of *covalence* of the HB interaction in water crystals.[33] We have now demonstrated

0947-6539/00/0624-4544 $ 17.50+.50/0 *Chem. Eur. J.* **2000**, *6*, No. 24

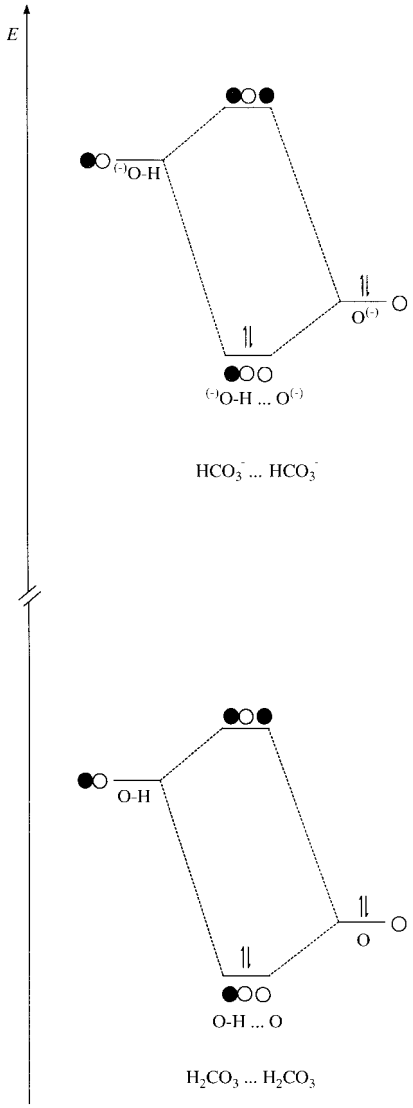

Scheme 5. Orbital combination in the cases of a chain of H_2CO_3 neutral molecules and of HCO_3^- anions. Note how the only difference between the two diagrams is the shift towards less stable energies of the orbitals of the HCO_3^- anion relative to those of the H_2CO_3 neutral molecule.

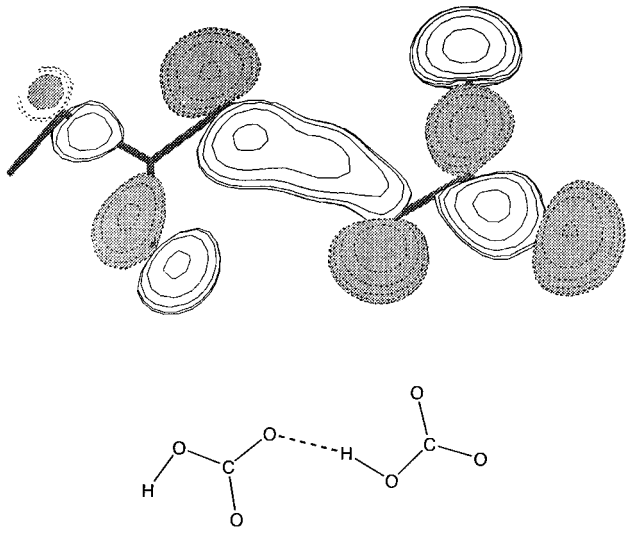

Figure 6. Top: Plot of the dimer orbital closest in shape to that of a bonding orbital associated to a O–H···O hydrogen-bond interaction. Due to the lack of axial symmetry of the molecule, the shape of the orbital in the proton-acceptor fragment does not show the typical shape of an O–H σ * expected in a perfectly collinear O–H···O arrangement. Notice the non-negligible overlap. The orientation of the dimer is given below. The curves correspond to 0.1 a.u..

that *the energetically unstable CHAIN dimers also show the same type of orbital combination, that is, some degree of covalence.* Therefore, the presence of covalence is not sufficient to turn the balance of the energetic factors towards stability but explains why the CHAIN motif is such a recurrent packing motif: though unstable with respect to dissociation in the absence of the counterions, the $^{(-)}$O–H···O$^{(-)}$ CHAIN (and RING, of course) formation is accompanied by the charge-transfer contribution to the total energy.

Another important property of charge transfer and polarisation is associated with the charges of the O–H group: upon formation of the short $^{(-)}$O–H···O$^{(-)}$ contact in the tetraionic units, there is an increase of 0.08 e^- on the O atom of the –OH group, and a decrease of 0.13 e^- of the H atom of the same group. The same trend was observed in the crystal, with a similar size of charge polarisation. The overall effect is a decrease in the number of electrons on the –OH group in agreement with the well-established shift of the vibrational frequencies of the –OH group involved in a $^{(-)}$O–H···O$^{(-)}$ interaction. It is interesting to note that the same kind of polarisation of the –OH group is found in the isolated HCO_3^- dimer whether at the geometry of the tetraionic unit or of the crystal. Hence, the presence of a vibrational shift is not, per se, a manifestation of a stable hydrogen-bonding interaction.

We have also carried out a critical-point analysis of the electronic density of the tetraionic unit, using Bader's quantum theory of atoms in molecules (QTAM).[34] Figure 7 shows the presence of a (3, –1) bond critical point computed at the MP2/6–31++G(d) level along the H···O path in the HCO_3^- dimer at any value of the H···O distance, including that observed in the $NaHCO_3$ crystal.[35] The critical point is present also in the $Na_2(HCO_3)_2$ tetraionic unit whether at the observed or optimised geometry. The properties of that H···O critical point (density and Laplacian) in the anionic CHAIN dimer are similar to those in the neutral CHAIN dimer. In addition, a clear Na···O bond path with a bond critical point is observed in the $Na_2(HCO_3)_2$ tetraionic unit both at crystal and optimised geometries. This critical point would indicate the presence of a bond between the negative oxygens of the anions and the cations. It is worth recalling, however, that critical points in the absence of a bond have been observed before. For instance, some intramolecular O···O or CH···HC contacts.[36] Besides, the presence of bond critical points with a bond path connecting the anions, such as in the LiF crystalline salt,[37] is well known, although it is clearly associated with the presence of repulsive interactions.

In summary, crystalline $NaHCO_3$ is stable because $Na^+\cdots HCO_3^-$ interactions (over)compensate for the +/+ and –/– repulsions. For example, the crystal is similar in many of its basic properties to an NaCl crystal, except for the peculiarity that the global $HCO_3^-\cdots HCO_3^-$ interactions are less repulsive than $Cl^-\cdots Cl^-$ interactions, and have a strong directional

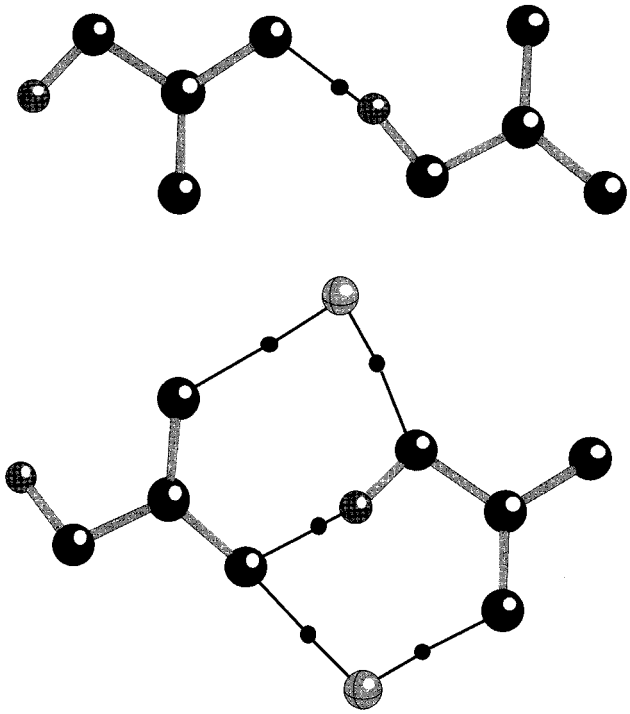

Figure 7. The H···O critical-point computed at the MP2/6–31++G(d) level when the dimer is placed at the distance observed in the $NaHCO_3$ crystal. All intermolecular (3, –1) bond critical points are shown: top, without cations, bottom, with the two Na^+ cations. The ions are distributed as in the observed crystal structure.

character caused by the need for the anions to optimise the $^{(-)}O–H\cdots O^{(-)}$ interactions. Even if the $^{(-)}O–H\cdots O^{(-)}$ interactions cannot bind the anions in the CHAIN motif they maintain the same directional properties as the hydrogen bonds and can thus be usefully employed in crystal engineering strategies.

One may wonder, at this point, why the RING, although more stable than the CHAIN motif, is not the packing motif of choice (see Table 1). Clearly, the answer must be found in the overall packing energy, as this is the property that determines the existence of different forms for a given crystal: an observable polymorph, or packing arrangement, must correspond to a minimum of the crystal free energy.[38] Hence, interconversion between polymorphs requires that an energy barrier is overcome. In the case of the RING–CHAIN isomerism, even though the RING dimer is markedly more stable, CHAIN aggregation in the crystal also corresponds to a minimum energy for the crystal packing, as demonstrated by the existence of both packing motifs for the same anion in some of its crystals (although no actual RING–CHAIN polymorphs with the same cation are known). The presence of only one of these packing forms must be related, on the one hand, to kinetic factors, similar to those that control nucleation and growth of different crystal forms of neutral molecules, and, on the other hand, to the convolution of charge distribution with crystal periodicity. The CHAIN motif generates a very regular one-dimensional network of anions, bordered by $M^+\cdots O$ interacting cations, while the RING motif, which we can now regard as a *supramolecular dianion*, is more adequately described as formed of $(M^+)_2[(HA)_2]^{2-}$ units and clearly has very different packing requirements. In the following section we will illustrate a new example of a RING–CHAIN alternative pattern and discuss the energetics of the two dimers in a different crystalline environment.

The crystalline structures of $NaHC_5O_5\cdot H_2O$, $RbHC_5O_5$ and $CsHC_5O_5$ and a comparison of the HB motifs: The two alternative CHAIN and RING motifs, which are known for the pair $NaHCO_3$ and $KHCO_3$, are also observed in the hydrogen croconate salts $RbHC_5O_5$ (CHAIN) and $CsHC_5O_5$ (RING), while, as discussed above, only the CHAIN motif has (as yet) been observed for all salts of hydrogen oxalates and for the hydrogen squarates salts of alkali cations. The two anhydrous salts $RbHC_5O_5$ (CHAIN) and $CsHC_5O_5$ (RING) will be discussed together, while the hydrated salt $NaHC_5O_5\cdot H_2O$, which shows a distorted CHAIN motif, will be treated separately. The sizes of the $RbHC_5O_5$ (CHAIN) and $CsHC_5O_5$ (RING) systems make them amenable to ab initio calculations (see next section).

The crystal structure of $RbHC_5O_5$[16] (Figure 8) is characterised by the presence of a chain of hydrogen croconate anions in "*anti*" conformation. The Rb^+ cation is encapsulated in the niche formed by three $HC_5O_5^-$ anions and interacts with oxygen atoms lone pairs, with Rb–O distances in the range 2.886(7)–2.958(8) Å. In contrast to the hydrogen squarates of Cs^+ and Rb^+, which are isomorphous,[39] $CsHC_5O_5$ is different

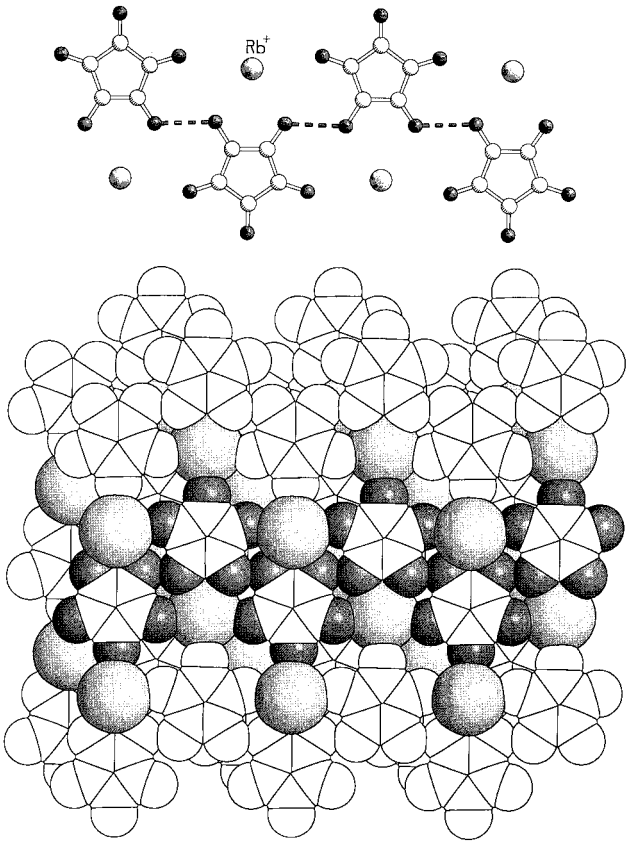

Figure 8. Top: The CHAIN motif in crystalline $RbHC_5O_5$. Bottom: Space-filling representation of the ion packing in $RbHC_5O_5$. The large shaded spheres represent the Rb^+ cations and the dark shaded atoms are the oxygen atoms.

0947-6539/00/0624-4546 $ 17.50+.50/0 *Chem. Eur. J.* **2000**, *6*, No. 24

from $RbHC_5O_5$, showing the presence of RING dimers (see Figure 9). The $^{(-)}O{-}H\cdots O^{(-)}$ separations are 2.443(8) Å in $RbHC_5O_5$ and 2.504(6) Å in $CsHC_5O_5$. In addition to this, $CsHC_5O_5$ has a short $^{(-)}O\cdots O^{(-)}$ contact of 2.897(6) Å bridged in a chain by $Cs^+\cdots O$ interactions (see Figure 9).

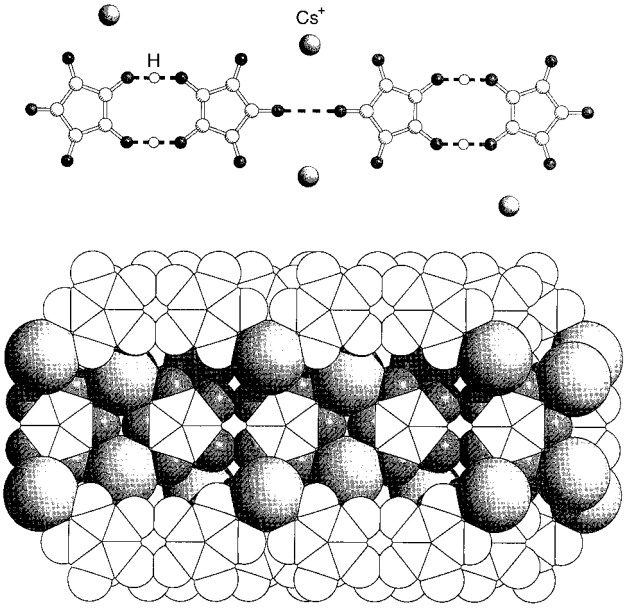

Figure 9. Top:The RING motif in crystalline $CsHC_5O_5$. Bottom: Space-filling representation of the ion packing in $CsHC_5O_5$. Note how the cyclic dimers also form short $^{(-)}O\cdots O^{(-)}$ contacts "bridged" by the Cs^+ cations (large shaded spheres). Dark shaded atoms are the oxygen atoms. The hydrogen atom involved in the $^{(-)}O{-}H\cdots O^{(-)}$ interaction, although not observed, has been added to the top drawing to distinguish this interaction from the $^{(-)}O\cdots O^{(-)}$ one.

The structure of $NaHC_5O_5\cdot H_2O$ is also of some interest in this context. Figure 10 shows the CHAIN motif in this hydrated crystal. The two interactions are slightly different in $O\cdots O$ separations [2.535(6), 2.457(5) Å] although within the range observed for other anionic chains (see hydrogen squarate in Table 1). The *anti* chain in $RbHC_5O_5$ is structurally very similar to those observed in the hydrogen squarate salts of Li^+, Na^+, K^+, Rb^+ and Cs^+.[39] The effect of hydration is one of the differences between the hydrogen croconate and hydrogen squarate families. In this latter family the CHAIN motif is maintained irrespective of the degree of hydration (two water molecules in $LiHC_4O_4$, one water molecule in $NaHC_4O_4$ and KHC_4O_4, no water in the Rb and Cs salts), while the $HC_5O_5^-$ salts show a much greater structural variability. The water molecules in $NaHC_5O_5\cdot H_2O$ point the O atoms towards the Na^+ cations, as expected, while the O–H groups form hydrogen-bonding interactions with the O atoms of the anions, thus acting as bridges between $HC_5O_5^-$ and Na^+. The coordination around Na^+ is roughly octahedral, each cation interacting with five $HC_5O_5^-$ oxygen atoms and one water oxygen atom. As in the case of $CsHC_5O_5$, there is a short $O\cdots O$ contact between $HC_5O_5^-$ anions belonging to adjacent chains [2.937(6) Å] corresponding to Na^+ bridges between anions.

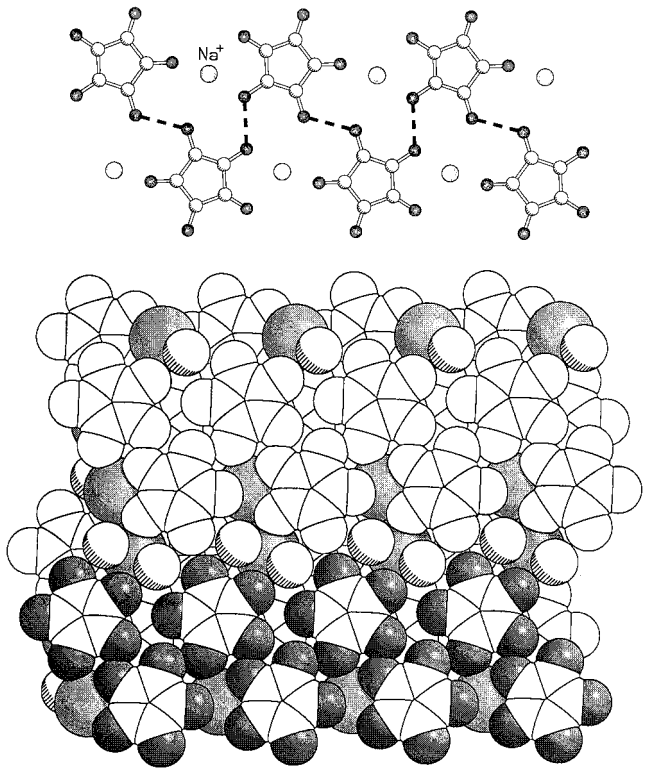

Figure 10. Top: Ball-and-stick representation of the distorted CHAIN motif in $NaHC_5O_5\cdot H_2O$ (small grey spheres represent the Na^+ cations). Bottom: Space-filling representation of the ion and water molecule packing in $NaHC_5O_5\cdot H_2O$, showing the layer of hydrogen croconate anions; the large shaded spheres underneath the anionic layer represent the Na^+ cations, and the dark shaded atoms are the oxygen atoms belonging to the anion. Hydrogen atoms are omitted.

Inter-anion RING–CHAIN interactions in $RbHC_5O_5$ and $CsHC_5O_5$ and the difference in energy between the two motifs: In this section we report the results of a computational investigation of the three fundamental motifs involving the O atoms and the –OH groups in the two salts $RbHC_5O_5$ and $CsHC_5O_5$, namely the Cs-bridged $^{(-)}O\cdots O^{(-)}$ contact in $CsHC_5O_5$, the $^{(-)}O{-}H\cdots O^{(-)}$ RING motif in $CsHC_5O_5$ and the $^{(-)}O{-}H\cdots O^{(-)}$ CHAIN motif in $RbHC_5O_5$. The results of the calculations carried out on tetraionic units formed by two alkali cations and two $HC_5O_5^-$ anions in the experimental geometry (see Experimental Section) are summarised in Table 3 and should be compared with the data discussed above in the cases of hydrogen carbonate and hydrogen oxalate anions.

One can see that the model systems constructed with two cations and two anions in the experimental orientation are stable. While all *homoionic* interactions are (expectedly) destabilising, the destabilisation is very small in the case of the RING motif. This result is in keeping with the results

Table 3. Interaction energies in Rb HC_5O_5 and Cs HC_5O_5 [kcal mol^{-1}].

	Cation–Cation	Anion–Anion	Whole motif
Cs HC_5O_5 $O^-\cdots O^-$	50.7	54.5	–205.9
Cs HC_5O_5 RING	23.2	0.7	–201.6
Rb HC_5O_5 CHAIN	45.8	41.6	–214.3

discussed above. As in the cases of the hydrogen carbonate and hydrogen oxalate anions the RING motif appears to be much less destabilising than the CHAIN motif (0.70 versus 41.60 kcal mol^{-1}). Remarkably, the *non-HB* $^{(-)}O\cdots O^{(-)}$ contact and the $^{(-)}O{-}H\cdots O^{(-)}$ CHAIN in $RbHC_5O_5$ have similar energetics; this indicates that the possible shielding effect, created by the hydrogen atom on the negatively charged $O^{(-)}$ atoms, is not sufficient to change the overall repulsive nature of the interanion interactions. The formation of an interatomic $^{(-)}O\cdots O^{(-)}$ separation slightly shorter than van der Waals distance (3.00 Å) is a manifestation of the electrostatic compression arising from strongly attractive forces between next-neighbours $Cs^+\cdots HC_5O_5^-$; these attractive forces overcompensate next-neighbour $HC_5O_5^-\cdots HC_5O_5^-$ repulsive forces and allow neighbouring atoms, *in spite of the like charge carried by the fragments*, to get much closer than in the case of neutral atoms.

Similar combinations of "unquestionably repulsive" short interanion $^{(-)}O\cdots O^{(-)}$ contacts and of $^{(-)}O{-}H\cdots O^{(-)}$ interactions are present in other alkali earth carboxylate salts, such as $Sr(HCOO)_2$[40a] (O···O 2.776–2.783 Å), $Ca(HCOO)_2$[40b] (2.816 Å) and $Li(C_7H_7O_2)$ (2.671–2.710 Å).[40c] It is worth recalling that the $O^{(2-)}\cdots O^{(2-)}$ separations in binary ionic oxides are in the range 2.42–2.56 Å.[41] Other examples of *charge-compressed* intermolecular interactions are those afforded by systems that form interanionic π-stacking interactions in the solid state.[39]

In summary, the computations in the case of the hydrogen croconates, although less detailed than those involving the hydrogen carbonate anion, confirm that the RING motif is energetically favoured over the isomeric linear CHAIN motif. The observation of both types of packing motifs, in spite of the energetic difference, lends further support to the idea that the "loss" of energy in the formation of CHAINs over RINGs ought to be compensated by a gain in attractive *heteroionic* terms. Although the different nature of the cations prevents direct comparison, it is noteworthy that the total energy of the CHAIN model in crystalline $RbHC_5O_5$ is more negative than that of the RING in $CsHC_5O_5$ (−214.3 versus −201.6 kcal mol^{-1}). This balance may, of course, yield different results in other ambients (but also in the crystal structures), for example, in solution where solvation energy needs to be taken into account.

Conclusion

The study of the HB interaction between anions has much to teach on the interplay between attractive and repulsive energetic components associated with the simultaneous presence of ions and of $O{-}H\cdots O$ bonding contacts. Our analysis lends further support to the idea that noncovalent interactions, their relative strength and their potentials as supramolecular tools have to be critically evaluated when passing from neutral to charged environments. The implications are considerable, not only in structural chemistry and crystal engineering, but also in biochemistry, as many biologically relevant interactions occur in electrolytic solutions and often occur between charged groups.

We have shown that the packing choice of small anions capable of HB interactions is critically dictated by two, not necessarily converging, factors: i) the optimisation of the network of interionic/intermolecular interactions with their directional requirements and ii) the balance between interionic attractive and repulsive forces. The conceptual relationship between attractive and repulsive forces and stabilising and destabilising interactions has been very clearly laid out by Dunitz and Gavezzotti in discussing the crystals of condensed aromatics.[42]

In this paper we have focussed our attention on the nature of $^{(-)}O{-}H\cdots O^{(-)}$ interactions between anions and on their role in the construction of the crystal edifice of HA^- anion salts. The problem has been tackled by means of database investigation, full ab initio treatment and preparation of novel systems and further structural studies.

The main points of the database study can be summarised as follows:

1) In the families of salts formed upon monodeprotonation of carbonic, oxalic, squaric and croconic acids RING and/or CHAIN motifs are observed for the $^{(-)}O{-}H\cdots O^{(-)}$ interactions.
2) RING dimers are known for hydrogen carbonates (with the exception of $NaHCO_3$), while the CHAIN is the only packing motif thus far observed for hydrogen oxalates.
3) Hydrogen squarates form both RINGs and CHAINs.
4) In the sparingly populated family of hydrogen croconate salts, the crystals of $NaHC_5O_5\cdot H_2O$ and of $RbHC_5O_5$ contain CHAINs of anions, while $CsHC_5O_5$ contains RING of anions.

The interaction between hydrogen carbonates in vacuum has been studied by investigating the change in the various energetic terms as the anions (OH^-, Cl^-, and HCO_3^-) approach, in other words, as the distance between two anions is decreased.

The following conclusions have been reached:

5) At large separations the $^{(-)}O{-}H\cdots O^{(-)}$ interaction between the anions is dominated by repulsive electrostatic forces due to the like charges, that is, the hydrogen carbonate anions studied here behave as spherical Cl^- ions and repel each other strongly.
6) At shorter separations ($H\cdots O < 2.5$ Å), however, the electrostatic term of the $^{(-)}O{-}H\cdots O^{(-)}$ interaction changes in nature and turns from positive into negative, because the positive charge carried by the H atom of the OH system is felt by the approaching $O^{(-)}$ terminus only at short distance.
7) This is observed for both types of geometries: the CHAIN and the RING. In the latter case, however, the effect is doubled because of the formation of two equivalent $^{(-)}O{-}H\cdots O^{(-)}$ interactions.
8) In spite of this, the overall energy of the anion aggregate remains positive. In other words, isolated CHAIN and RING dimers remain unstable with respect to dissociation, albeit with an energy that is much smaller than one could expect simply on the basis of point charges.

On passing from the vacuum to the condensed phase, the following observations have been made in the cases of hydrogen carbonate and/or hydrogen oxalate anions:

0947-6539/00/0624-4548 $ 17.50+.50/0 *Chem. Eur. J.* **2000**, *6*, No. 24

1) In solution, within a cage of solvent molecules, the CHAIN dimer dissociates spontaneously, while the RING dimer, once formed, is energetically stable.
2) The evolution over time of the CHAIN and RING systems confirms that the CHAIN dimer tends to dissociate, while the RING dimer should live long enough to be observable with solution techniques, such as NMR spectroscopy. The RING dimer can be expected to be the motif of choice of HA^- anions (at least in nonaqueous solutions).
3) Charge-density polarisation does not appear to play a significant role on passing from the vacuum to the solid state; irrespective of the models used to describe the hydrogen oxalate anion, only small changes in the charge distribution over the $^{(-)}O{-}H\cdots O^{(-)}$ system have been observed, depending on the type of computational approach.
4) In the Madelung field of the crystal, the effect of polarisation on the energetics of the CHAIN dimer is small and not sufficient to alter the strongly repulsive nature of the overall interaction. This is not so for the RING dimer, which becomes energetically stable within the crystal field generated by the surrounding ions.

We have also shown that the $^{(-)}O{-}H\cdots O^{(-)}$ interaction possesses many of the features of neutral hydrogen bonds, such as the vibrational shift associated with weakening of the O–H bond and a small, but detectable, "covalent" component, due to the charge transfer from the proton-donor anion to the proton-acceptor anion in the isolated dimer, similar to that observed in dimers of neutral molecules. This charge transfer component is only possible when the anions are brought in close proximity by the effect of cation–anion attractions. In addition, the calculation at the MP2/6–31++G(d) level of the $H\cdots O$ path in the HCO_3^- dimer shows the presence of a bond critical point at any value of the $H\cdots O$ distance. Therefore, all these features, shared with neutral hydrogen bonds, are indeed diagnostic of the presence of a $^{(-)}O{-}H\cdots O^{(-)}$ interaction but not of an overall stability of the anion aggregate.

We have integrated our knowledge of the structures of small organic HA^- anions with the structural analysis of new hydrogen croconate salts. We have shown that:

1) The crystals of $RbHC_5O_5$ and $CsHC_5O_5$ contain the two alternative CHAIN and RING motifs. Calculations carried out on the two motifs show the same trend in energy as discussed above (i.e., the RING is more stable than the CHAIN). One may speculate on the effect of cation size: the slightly larger Cs^+ cation might be too large to be accommodated in the *tweezer* system formed by the CHAIN causing the equilibrium to shift towards the RING motif.
2) The structural analysis also provides the important notion that $^{(-)}O\cdots O^{(-)}$ contact distances, shorter than in neutral systems, are a manifestation of the *electrostatic compression* arising from attractive next-neighbour anion–cation interactions, which largely overcompensate the combined effect of next-neighbour anion–anion and cation–cation repulsions and allow deeper penetration into the repulsive wall of neighbouring atoms.

We concluded our preliminary communication with the statement: "if a bond between two atoms/molecules/ions is taken as anything that requires energy to be broken (whether large or small amount of energy does not matter) then the $^{(-)}O{-}H\cdots O^{(-)}$ interaction cannot be considered a bond because the ionic chains (or dimers) would 'fall apart' if the cations were removed." We believe that this is in exact accord with Linus Pauling's definition[12] of a chemical bond: "*There is a chemical bond between two atoms or group of atoms in case that the forces acting between them are such as to lead to the formation of an aggregate with sufficient stability to make it convenient for the chemist to consider it as an independent molecular species*" in which the emphasis is on the concept of stability.

The "breakdown of strength–length analogy" is nothing more than the recognition that $^{(-)}O{-}H\cdots O^{(-)}$ interactions are not energetically determinant in the cohesion of a hydrogen-bonded salt, whilst they are responsible for the spatial organisation of the anions. On the other hand, by arranging anions in CHAINs or RINGs, $^{(-)}O{-}H\cdots O^{(-)}$ interactions contribute to cohesion by reducing interanion repulsions, that is, by decreasing the $-/-$ term within the overall balance of $+/-$, $-/-$ and $+/+$ attractions and repulsions. $^{(-)}O{-}H\cdots O^{(-)}$ interactions are transferable from packing to packing, are predictable and reproducible (very robust synthons indeed), they have many of the features of neutral hydrogen bonds (such as characteristic IR and NMR spectra), they are even generally shorter than neutral bonds, but they are not sufficient to keep ions together.

In the end, this study has increased our awareness of the concept of supramolecular bonding in crystals. On a supramolecular scale,[43] and, indeed, on a crystal engineering scale[9, 10] where aggregates of molecules and ions interacting through noncovalent bonds become periodical supermolecules, the perception of *bonding interactions* needs to be broadened. One may think of rephrasing Pauling in supramolecular terms: *"there is a supramolecular chemical bond between two molecules or ions in case that the forces acting between them are such as to lead to the formation of an aggregate with sufficient stability to make it convenient for the supramolecular chemist/crystal engineer to consider it as an independent supramolecular species"*. In the case addressed in this paper, the stable aggregate can only be formed by the anions in the presence of the cations. The universality of Linus Pauling is in that he has given us the tools to understand these complex situations.

Experimental Section

Croconic acid was purchased from Aldrich. The hydrogen croconate salts of Rb^+, Cs^+ and Na^+ were obtained by direct reaction of croconic acid with the appropriate hydroxide. Croconic acid (50 mg, 0.35 mmol) was dissolved in of RbOH, CsOH or NaOH (10 mL, 0.035 mol). Crystals suitable for X-ray diffraction were obtained by slow evaporation of the water solutions.

Crystallography: Crystal data and details of measurements for species $CsHC_5O_5$, $RbHC_5O_5$ and $NaHC_5O_5\cdot H_2O$ are reported in Table 4. All non-H atoms were refined anisotropically except the water oxygens in $CsHC_5O_5$. The structure of $RbHC_5O_5$ was already known and has been redetermined in order to obtain more accurate structural parameters.

Table 4. Crystal data and details of measurements for $CsHC_5O_5$, $RbHC_5O_5$ and $NaHC_5O_5 \cdot H_2O$.

	$CsHC_5O_5$	$RbHC_5O_5$	$NaHC_5O_5 \cdot H_2O$
formula	C_5HCsO_5	C_5HRbO_5	$C_5H_3NaO_6$
M_w	273.97	226.53	182.06
T [K]	273(2)	223(2)	223(2)
system	monoclinic	monoclinic	triclinic
space group	$I2/m$	$P2_1/c$	$P\bar{1}$
a [Å]	5.296(2)	7.692(2)	5.579(3)
b [Å]	14.804(5)	10.433(3)	7.764(4)
c [Å]	8.496(3)	7.765(2)	7.882(5)
α [°]	90	90	114.37(5)
β [°]	96.78(3)	101.45	97.16(5)
γ [°]	90	90	85.46(5)
V [Å^3]	661.4(4)	610.7(3)	308.4(3)
Z	4	4	2
$F(000)$	504	432	184
transmission min/max	0.58/1.00	0.67/1.00	0.88/1.00
$\mu(Mo_{K\alpha})$ [mm^{-1}]	5.564	8.069	0.240
measured reflns	649	1152	1162
unique reflns	608	1068	1063
parameters	55	100	85
GOF on F^2	1.074	0.978	0.931
$R1$ [on F, $I > 2\sigma(I)$]	0.0332	0.0622	0.0751
$wR2$ (on F^2,all data)	0.0805	0.1904	0.2259

Common to all compounds: $Mo_{K\alpha}$ radiation, $\lambda = 0.71069$ Å, graphite monochromator, Ψ-scan absorption correction. All non-H atoms were refined anisotropically. No H atom positions were observed, except for one H atom involved in the two $^{(-)}O{-}H\cdots O^{(-)}$ interactions in $NaHC_5O_5 \cdot H_2O$: the hydrogen was found on an inversion centre, with an occupancy factor of 0.50. The computer program SHELXL 97[44a] was used for structure solution and refinement. The computer program SCHAKAL 97[44b] was used for all graphical representations. Crystallographic data (excluding structure factors) for the structures reported in this paper have been deposited with the Cambridge Crystallographic Data Centre as supplementary publication nos. CCDC-144408, CCDC-144409 and CCDC-144410. Copies of the data can be obtained free of charge on application to CCDC, 12 Union Road, Cambridge CB2 1EZ, UK (fax: (+44) 1223-336-033; e-mail: deposit@ccdc.cam.ac.uk). .

Database analysis: Data were retrieved from the October 1999 version of the CSD[18a] and from the ICSD.[18b] The CSD data were searched for all crystal structures with an exact match between chemical and crystallographic connectivity on fragments designed with the QUEST software. All entries were manually screened. The presence of experimentally located H atoms was required for a bona fide identification of the $^{(-)}O{-}H\cdots O^{(-)}$ interactions, but no distinction between X-ray and neutron structures was performed.

Energetic computations: Ab initio calculations were carried out with the HF/6–31+G(2d,2p) Hartree–Fock method and the 6–31+G(2d,2p) set and with MP2/6–31+G(2d,2p), which refers to computations done by using the same basis set and the second-order Møller–Plesset method.[45] The computer program Gaussian 94 was used.[45] The aim in the CPFGA (crystal packing functional group analysis) analysis was not to compute the actual crystal packing of a given molecule, but to understand the reasons for the packing by looking at the packing energy as the sum of the interaction energy between pairs of molecules, and rationalising the energy involved in each pair in terms of the intermolecular bonds made among the functional groups of these molecules.[46] For ionic interactions the Hartree–Fock method is capable of providing results close to the second-order Møller–Plesset (MP2) or better methods, in any case of the right order and sign. The HF method has been used in conjunction with the 6–31+G(2d,2p) basis set for the atoms of the first and second rows. For all the other atoms we used the LANL2DZ core potentials, while the valence electrons were described by using the LANL2DZ basis complemented by two sets of polarisation functions, thus affording a similar precision in the description of the valence electrons of all atoms. The distributed multipole analysis of the electrostatic potential was done up to the quadrupole terms by using the procedure introduced by Stone.[47]

The $(3,-1)$ bond critical-point search and bond path assignment were carried out by using a version of the AIMPAC package.[48] Mathematically a $(3,-1)$ bond critical point is an electron-density region in which the density gradient is equal to zero and the Hessian presents two negative and one positive eigenvalues.[34] Bond critical points associated with intermolecular interactions have a Laplacian (defined as the sum of the Hessian eigenvalues) larger than zero, small values of the density at the critical point and small values of the absolute value of the lowest and highest eigenvalues of the Hessian. All the intermolecular critical points found here share these characteristics, typical of hydrogen bonds and van der Waals bonds.

Details on the first principle Carr–Parrinello dynamic simulations: A detailed description of the Carr–Parrinello method can be found in several publications.[30] The calculations on the charged dianions were performed isolated supercells of dimensions $a = 14$ Å, $b = 9$ Å and $c = 7$ Å for the RING dianion, $a = 7$ Å, $b = 9$ Å and $c = 16$ Å for the CHAIN dianion and $a = 18$ Å, $b = 12$ Å and $c = 12$ Å for the solvated RING dianion. We used the generalised gradient-corrected approximation of spin-dependent density functional theory (DFT-LSD), following the prescription of Becke and Perdew. The electronic wave functions were expanded in plane waves up to a kinetic energy cutoff of 70 Ry for the gas-phase dianions. Martins–Troullier norm-conserving pseudopotentials were also used in all atoms.[49] The dynamical simulations used a time step of 0.12 fs and the fictitious mass of the Carr–Parrinello Lagrangian was set to 700 au.[48] The initial configurations were taken as indicated in the following: the HF/6–31G++G(2d,2p) optimised structure for the RING dimer, a configuration with $O\cdots H = 2.0$ Å for the CHAIN dimer, and the HF/6–31+G optimised structure for the solvated RING dimer. The gas-phase dimers were allowed to evolve during 1 ps in order to achieve vibrational equilibration, and the simulations were followed for 3–4 ps at an average temperature of 300 K. Because of the large computational cost of the solvated dianion, the PW cutoff was reduced to 50 Ry and the simulations were run for 0.6 ps at an average temperature of 300 K. Although the dynamical results of this solvated cluster will be only qualitative, we believe that they can account for a possible tendency of the solvated dianion towards dissociation. In fact, while we found for the gas-phase RING dimer a tendency towards dissociation at the initial equilibration stages of the dynamics, such a dissociation tendency was not observed in the solvated dimer even in the initial equilibration time.

CRYSTAL calculation: The CRYSTAL package[32] has been used to perform ab initio periodic computations on the experimental geometry of the $NaHCO_3$, $KHCO_3$ and KHC_2O_4 crystals. The Hartree–Fock Hamiltonian was used and a gaussian basis set, which is the 6–31G(d,p) for the C, O and H atoms, and the 86–511G(d) basis for Na (the K atoms were substituted for Na in these computations). The dimer was computed in CRYSTAL as a cluster, in other words without periodic boundary conditions, but with the same basis set employed in the whole crystal. In all computations, whether starting from observed or model systems, neutron-derived positions for the H atoms were used.

Note added in proof: While this paper was being processed, two other communications on this subject have been published.[14b, c] We trust that our study addresses all significant issues raised in these two papers.

Acknowledgements

D.B. and F.G. thank M.U.R.S.T. (project *Supramolecular Devices*), the University of Bologna (project *Innovative Materials*) and the University of Sassari for financial support. J.J.N. thanks DGES (project PB98-1166-C02-02) and CIRIT (1999SGR 00046) for their support, and CESCA-CEPBA for the allocation of computer time. C.R. thanks "Ministerio de Educacion y Ciencia" for her research contract. Prof. F. Zerbetto and Dr. M. Mascal are thanked for many useful discussions.

[1] G. A. Jeffrey, *An Introduction to Hydrogen Bonding*, Oxford University Press, New York, **1997**.

[2] a) M. C. Etter, *Acc. Chem. Res.* **1990**, *23*, 120; b) J. Bernstein, R. E. Davis, L. Shimoni, N.-L. Chang, *Angew. Chem.* **1995**, 107, 1689; *Angew. Chem. Int. Ed. Engl.* **1995**, *34*, 1555.

  0947-6539/00/0624-4550 $ 17.50+.50/0

[3] G. R. Desiraju, *Angew. Chem.* **1995**, *107*, 2541; Angew. *Chem. Int. Ed. Engl.* **1995**, *34*, 2311.

[4] M. S. Gordon, J. H. Jensen, *Acc. Chem. Res.* **1996**, *29*, 536, and references cited therein.

[5] H. Umeyama, K. Morokuma, *J. Am. Chem. Soc.* **1977**, *99*, 1316.

[6] a) G. Gilli, F. Bellucci, V. Ferretti, V. Bertolasi, *J. Am. Chem. Soc.* **1989**, *111*, 1023; b) V. Bertolasi, P. Gilli, V. Ferretti, G. Gilli, *Chem. Eur. J.* **1996**, *8*, 925, and references cited therein.

[7] See for example: a) M. Meot-Ner (Mautner) *J. Am. Chem. Soc.* **1984**, *106*, 1257; b) M. Meot-Ner (Mautner), L. W. Sieck, *J. Am. Chem. Soc.* **1986**, *108*, 7525.

[8] a) D. Braga, F. Grepioni, *J. Chem. Soc. Dalton Trans.* **1999**, 1; b) M. W. Hosseini, A. De Cian, *Chem. Commun*. **1998**, 727; c) L. Brammer, D. Zhao, F. T. Ladipo, J. Braddock-Wilking, *Acta Crystallogr. Sect. B* **1995**, *51*, 632; d) C. B. Aakeröy, *Acta Crystallogr*. *Sect. B* **1997**, *53*, 569; e) D. Braga, F. Grepioni, *Chem. Commun*. **1996**, 571; f) D. Braga, F. Grepioni, *New J. Chem.* **1998**, 1159.

[9] a) *Crystal Engineering: from Molecules and Crystals to Materials* (Eds: D. Braga, F. Grepioni, A. G. Orpen), Kluwer Academic, Dordrecht, **1999**; b) D. Braga, F. Grepioni, G. R. Desiraju, *Chem. Rev.* **1998**, *98*, 1375.

[10] D. Braga, F. Grepioni, *Acc. Chem. Res.* **2000**, *33*, 601.

[11] a) D. Braga, F. Grepioni, E. Tagliavini, J. J. Novoa, F. Mota, *New. J. Chem.* **1998**, 755; b) J. J. Novoa, I. Nobeli, F. Grepioni, D. Braga, *New J. Chem.* **2000**, *24*, 5.

[12] L. Pauling, *The Nature of the Chemical Bond*, Cornell University Press, Ithaca, NY, **1960**, p. 6.

[13] D. Braga, F. Grepioni, J. J. Novoa, *Chem. Commun.* **1998**, 1959.

[14] a) T. Steiner, *Chem. Commun.* **1999**, 2299; b) M. Mascal, C. E. Marajo, A. J. Blake, *Chem. Commun.* **2000**, 1591; c) P. Macchi, B. B. Iversen, A. Sironi, B. C. Chokoumakas, F. K. Larsen, *Angew. Chem.* **2000**, *112*, 2831; *Angew. Chem. Int. Ed.* **2000**, *39*, 2719.

[15] D. Braga, F. Grepioni, J. J. Novoa, *New J. Chem.*, in press.

[16] The crystal structure of $RbHC_5O_5$ has been redetermined in order to obtain a more accurate data set; previous determination: N. C. Baezinger, D. G. Williams, *J. Am. Chem. Soc.* **1966**, *88*, 689.

[17] a) J. J. Novoa, M. Deumal, *Mol. Cryst. Liq. Cryst*. **1997**, *305*, 143; b) M. Deumal, J. Cirujeda, J. Veciana, M. Kinoshita, Y. Hosokoshi, J. J. Novoa, *Chem. Phys. Lett.* **1997**, *265*, 190; c) *Implications of Molecular and Materials Structure for New Technologies* (Eds: J. J. Novoa, F. Allen, J. Howard), Kluwer Academic, Dordrecht, **1999**; d) C. Lee, G. Fitzgerald, M. Planas, J. J. Novoa, *J. Phys. Chem.* **1996**, *100*, 7398.

[18] a) F. H. Allen, O. Kennard, *Chem. Des. Autom. News* **1993**, *8*, 31; b) Inorganic Crystal Structure Database (ICSD), Fachinformationszentrum (FIZ) Karlsruhe and Gmelin Institut, Release 99/2.

[19] a) L. Leiserowitz and G. M. J. Schmidt, *J. Chem. Soc. A* **1969**, 2372; b) L. Leiserowitz *Acta Crystallogr. Sect B* **1976**, *32*, 775; c) Z. Berkovitch-Yellin, L. Leiserowitz, *J. Am. Chem. Soc.* **1982**, *104*, 4064.

[20] O. N. Ventura, J. B. Rama, L. Turi, J. J. Dannenberg, *J. Phys. Chem*. **1995**, *99*, 131.

[21] a) A.Gavezzotti, *Chem. Eur. J.* **1999**, *5*, 567; b) A.Gavezzotti, G. Filippini, J. Kroon, B. P. van Eijck, P. Klewinghaus *Chem. Eur. J.* **1997**, *3*, 893.

[22] F. H. Allen, W. D. S. Motherwell, P. R. Raithby, G. P. Shields, R. Taylor, *New J. Chem.* **1999**, 25.

[23] I. Nahringbauer, *Acta Crystallogr. Sect. B* **1970**, *24*, 453.

[24] a) L. Turi, J. J. Dannenberg, *J. Am. Chem. Soc.* **1993**, *97*, 12197; b) L. Turi, J. J. Dannenberg, *J. Am. Chem. Soc.* **1994**, *116*, 8714.

[25] J. C. Derrissen, P. H. Smit *Acta Crystallogr. Sect. B* **1974**, *30*, 2240.

[26] D. Braga, F. Grepioni, P. Sabatino, G. R. Desiraju, *Organometallics* **1994**, *13*, 3532.

[27] B. D. Sharma, *Acta Crystallogr*. **1965**, *18*, 818.

[28] I. C. Hayes, A. J. Stone, *Mol. Phys*. **1984**, *53*, 83; computed by using the Cadpac 6.1 , included as part of the Unichem 4.1 suite.

[29] This is evidently the case in the HCO_3^- anion, but is also found in the $HC_2O_4^-$ anion, whose charges in the $-COO^{(-)}$ end are: C = 0.77 e$^-$ and O = −0.73 e$^-$. However, one has to note that the charge in the −COOH end of the $HC_2O_4^-$ anion is not very different: C = 0.70 e$^-$, O = −0.62 e$^-$, and H = 0.34 e$^-$.

[30] a) R. Car, M. Parrinello, *Phys. Rev. Lett.*, **1985**, *55*, 2471; b) G. Galli, M. Parrinello in *Computer Simulation in Materials Science* (Eds: V. Pontikis, M. Meyer), Kluwer Academic, Dordrecht, **1991**.

[31] a) A. D. Becke, *J. Chem. Phys.* **1986**, *84*, 4524. b) J. P. Perdew, *Phys. Rev. B*, **1986**, *33*, 8822.

[32] V. R. Saunders, R. Dovesi, C. Roetti, M. Causa, N. M. Harrison, R. Orlando, C. M. Zicovich-Wilson, CRYSTAL 98 User's Manual, University of Torino, Torino **1998**.

[33] Some amount of covalency was seen to be necessary to reproduce the experimental X-ray diffraction patters in ice, which was not possible to be reproduced by purely electrostatic (ionic) models. Covalency was accounted for by allowing the combination of the orbitals of the water fragments. E. D. Isaacs, A. Shukla, P. M. Platzman, D. R. Hamann, B. Barbiellini, C. A. Tulk, *Phys. Rev. Lett.* **1999**, *82*, 600.

[34] R. F. W. Bader, *Atoms in Molecule. A Quantum Theory*, Clarendon, Oxford, **1990**.

[35] V. G. Tsirelson, P. F. Zou, T.-H. Tang, R. F. W. Bader, *Acta Crystallogr Sect. A.* **1995**, *51*, 143.

[36] We have also seen the presence of bond critical points in other neutral-molecule – neutral-molecule repulsive interactions, linking the shortest two contacts, as in the case of two water molecules placed with the two oxygen atoms facing each other and the hydrogen pointing outwards from these oxygens, or in anion – anion interactions as in the case of the Cl^- dimer, at any distance between the two anions.

[37] a) J. Cioslowski, S. T. Mixon, *J. Am. Chem. Soc.* **1992**, *114*, 4382; b) J. Cioslowski, P. B. O'Connor, E. D. Fleishmann, *J. Am. Chem. Soc.* **1991**, *113*, 1086; c) J. Cioslowski, S. T. Mixon, W. D. Edwards, *J. Am. Chem. Soc.* **1991**, *113*, 1083.

[38] a) J. Dunitz, J. Bernstein, *Acc. Chem. Res.* **1995**, *28*, 193; b) J. Bernstein, R. J. Davey, J.-O. Henck, *Angew. Chem.* **1999**, *111*, 3646; *Angew. Chem. Int. Ed.* **1999**, *38*, 3440.

[39] D. Braga, C. Bazzi, F. Grepioni, J. J. Novoa, *New J. Chem*. **1999**, *23*, 577.

[40] a) W. Matsui, *Acta Crystallogr. Sect. B* **1978**, *34*, 2731; b) H.Fuess, N. Burger, J. W. Bats, *Z. Kristallogr.* **1981**, *156*, 219; c) S. Onuma, S. Shibata, *Fac. Sci. Shizuoka Univ*. **1978**, *12*, 45.

[41] J. E. Huheey, E. A. Keiter, R. L. Keiter, *Inorganic Chemistry,* 4th ed., Harper Collins, New York, **1993**.

[42] J. D. Dunitz, A. Gavezzotti, *Acc. Chem. Res.* **1999**, *32*, 677.

[43] J. M. Lehn, *Supramolecular Chemistry: Concepts and Perspectives*, VCH, Weinheim, **1995**.

[44] a) G. M. Sheldrick, *SHELXL 97, Program for Crystal Structure Determination*, University of Göttingen, Göttingen, Germany, **1997**; b) E. Keller, *SCHAKAL 97, Graphical Representation of Molecular Models*; University of Freiburg, Freidberg, Germany, **1997**.

[45] a) M. J. Frisch, G. W.Trucks, H. B Schlegel, P. M. W.Gill, B. G. Johnson, M. A. Robb, J. R. Cheeseman, T. Keith, G. A. Peterson, J. A. Montgomery, K. Raghavachari, M. A. Al-Laham, V. G. Zakrzewski, J. V. Ortiz, J. B. Foresman, J. Ciolowski, B. B. Stefanov, A. Nanayakkara, M. Challacombe, C. Y. Peng, P. Y. Ayala, W. Chen, M. W. Wong, J. L. Andres, E. S. Replogle, R. Gomperts, R. L. Martin, D. J. Fox, J. S. Binkley, D. J. Defrees, J. Baker, J. J. P. Stewart, M. Head-Gordon, C. Gonzalez, J. A. Pople, *Gaussian 94, Revision C.3*, Gaussian, Pittsburgh PA, **1995**; b) S. Huzinaga, *Gaussian Basis Sets for Molecular Calculations*, Elsevier, Amsterdam **1984**.

[46] a) J. J. Novoa, M. Deumal, *Mol. Cryst. Liq. Cryst*. **1997**, *305*, 143; b) M. Deumal, J. Cirujeda, J. Veciana, M. Kinoshita, Y. Hosokoshi, J. J. Novoa, *Chem. Phys. Lett.* **1997**, *265*, 190; c) J. J. Novoa in *Implications of Molecular and Materials Structure for New Technologies* (Eds.: F. Allen, J. Howard), Kluwer Academic, Dordrecht, **1999**.

[47] a) A. J. Stone, Chem. *Phys. Lett*. **1981**, *83*, 233; b) S. L. Price, A. J. Stone, *Chem. Phys. Lett*. **1983**, *98*, 419.

[48] F. Biegle-Koning, R. F. W. Bader, W.-H. Tang, *J. Comput. Chem*. **1982**, *3*, 317.

[49] N. Troullier, J. L. Martins *Phys. Rev. B.* **1991**, *43*, 1993.

Received: May 25, 2000 [F2515]